

PHYSICS OF FUSION FUEL CYCLES

J. RAND McNALLY, Jr. *Oak Ridge National Laboratory
Fusion Energy Division, P.O. Box Y, Oak Ridge, Tennessee 37830*

OVERVIEW

FUSION FUEL CYCLES

Received August 3, 1981

The evaluation of nuclear fusion fuels for a magnetic fusion economy must take into account the various technological impacts of the various fusion fuel cycles as well as the relative reactivity and the required betas, temperatures, and confinement times necessary for economic steady-state burns. The physics of the various fuel cycles [deuterium-tritium, catalyzed deuterium-deuterium (D-D), D-³He, D-⁶Li, and the exotic fuels: ³He-³He and the proton-based fuels p-⁶Li, p-⁹Be, and p-¹¹B] is reviewed. Topics considered include

1. fuel costs and required purity
2. tritium inventory, burnup, and recycle
3. ignition criteria
4. neutrons
5. condensable fuels and ashes
6. radiation losses
7. direct electrical recovery prospects
8. fissile breeding prospects.

The advantages and disadvantages of each fuel are also treated. The optimum fuel cycle from an overall standpoint of viability and potential technological considerations appears to be catalyzed D-D, which could also support smaller, relatively "clean," lean deuterium-rich ³He satellite reactors as well as fission reactors.

INTRODUCTION

Significant progress has been made toward achieving the physics goal of an ignited fusion fuel confined in a magnetic field. Whereas toroidal magnetic devices, as exemplified by the stellarator, were a factor of 10 billion away from this goal in 1958, the present achievements in the Princeton Large Torus (PLT) device (1978 to 1981) are only about a factor of

200 away from an ignition condition. Thus, it is opportune to review some of the physics of the various proposed fusion fuel cycles, to review their pros and cons regarding viability and technology, and to recommend an optimum fusion fuel economy on the basis of present knowledge.

Serious consideration of light element burning for energy release apparently was first made in 1946, when problems of achieving both high density arc plasmas and low density, magnetically confined plasmas were outlined briefly in a classified document prepared at the Los Alamos National Laboratory.¹ This work led eventually to the U.S. Sherwood project, which began about 1951 and was declassified along with other international disclosures of controlled fusion research at the 1958 Second Atoms for Peace Conference in Geneva, Switzerland.² Since that time, magnetically confined plasma research has been unclassified, whereas some of the inertial confinement research is still classified because of its apparent implications to thermonuclear weapons evaluations.

The first step in evaluating the potential technological impact of the development of fusion power is to examine the basic physics of possible fusion fuels and the criteria that govern the development of these fuel reactions for practical power sources. The principal approaches to the conceptualizing of fusion reactors to produce this power are discussed in an earlier paper by Baker et al.³

FUSION FUELS

The earliest detailed evaluations of light element burning were made by Bethe and von Weizsäcker in the late 1930s to explain the energy source of the sun and stars; these processes involved the very slow proton-proton cycle and the carbon cycle, both of which convert protons to alpha particles with about a 28-MeV energy release in each complete cycle.⁴ Such reactions are extremely unlikely to be used for man-made controlled thermonuclear energy release because of

1. the small nuclear cross sections for most reaction steps and the long confinement times

required in gravitational confinement of the reactants

2. the prohibitively large particle density required.

The fusion reactions of interest for generating controlled fusion energy release occur between two light nuclei, producing two or more product particles and a net energy release. Possible reactions include one or more isotopes of each of the first five elements (hydrogen, helium, lithium, beryllium, and boron). The reaction products include neutrons and nuclei of the light elements, with reaction energies in the range Q up to 22 MeV per event. The reaction energy is usually carried off as kinetic energy of the product particles, although some gamma rays are occasionally emitted.

Fusion reactions of primary interest and energy yields in million electron volts ($1 \text{ MeV} = 1.602 \times 10^{-13} \text{ J}$) are shown in Table I. The energy release in fusion can appear as neutron energy and/or as charged particle energy. Of special interest for various fusion reactions is the distribution of energy between the charged and uncharged particles. Except for center-of-mass motion effects and three body products the reaction product energy is inversely proportional to its mass (as shown in Table I). For presently envisioned magnetic fusion reactors, only the energy of the charged particles will be deposited within the plasma to compensate for various energy loss mechanisms and thus to sustain the fusion burn. Neutrons will escape from the reaction chamber and deposit their kinetic energy in a blanket surrounding the plasma, usually generating additional energy in the blanket (e.g., 4.8 MeV per ^6Li capture reaction). This energy will be recovered by a thermal energy conversion system. The charged-particle energy may also be recovered as heat, although direct conversion to electricity of some charged-particle energy may be possible. Some of the charged-particle energy escapes as radiation and is deposited at the first wall.

The charged-particle power release in a reacting plasma that has a constant electron density and selected fuel ion densities is given in Fig. 1 for several important reactions as a function of the kinetic temperature. These calculations are based on reaction probability tables of McNally et al.⁵ Supplementary tables are available in a report by Howerton.⁶ As shown here, the charged-particle energy releases of deuterium-based fuels are generally greater than those of the proton-based fuels. The deuterium-based fuels are thus more reactive, but they generate more neutrons (see Table I). One exception to this classification (i.e., deuterium-based versus proton-based) is the $^3\text{He}-^3\text{He}$ reaction, which involves "proton-rich" nuclides and generates only charged particles. Because of its very small reaction probability, $^3\text{He}-^3\text{He}$ is in

the class of "exotic" fuels along with the proton-based fuels.

The various fusion fuels may be designated as "classical," "conventional," or "exotic," as shown in Table II. The cost and purity of the different fusion fuels are given in Table III although it should be noted that tritium (and probably ^3He) fuel costs may be a one-time expenditure if predictions for excess tritium breeding prospects prove out.

Several fuel cycles based on the reactions listed in Table I are noteworthy:

TABLE I
Fusion Reactions

| Deutron-Based Fusion Fuels | |
|--|--|
| <u>Primary Reactions^a</u> | |
| $\text{D} + \text{T} \rightarrow \text{n} + ^4\text{He} + 17.586 \text{ MeV}$ (3.517 MeV) | |
| $\text{D} + \text{D} \rightarrow \text{p} + \text{T} + 4.032 \text{ MeV}$ (4.032 MeV) | |
| $\text{D} + \text{D} \rightarrow \text{n} + ^3\text{He} + 3.267 \text{ MeV}$ (0.817 MeV) | |
| $\text{D} + ^3\text{He} \rightarrow \text{p} + ^4\text{He} + 18.341 \text{ MeV}$ (18.341 MeV) | |
| $\text{D} + ^6\text{Li} \rightarrow 2^4\text{He} + 22.374 \text{ (22.374 MeV)}$ | |
| $\text{D} + ^6\text{Li} \rightarrow \text{p} + ^7\text{Li} + 5.026 \text{ MeV}$ (5.026 MeV) | |
| $\text{D} + ^6\text{Li} \rightarrow \text{n} + ^7\text{Be} + 3.380 \text{ MeV}$ (0.473 MeV) | |
| $\text{D} + ^6\text{Li} \rightarrow \text{p} + \text{T} + ^4\text{He} + 2.561 \text{ MeV}$ (2.561 MeV) | |
| $\text{D} + ^6\text{Li} \rightarrow \text{n} + ^3\text{He} + ^4\text{He} + 1.796 \text{ MeV}$ (~1.134 MeV) | |
| <u>Secondary Reactions</u> | |
| $\text{p} + \text{T} \rightarrow \text{n} + ^3\text{He} - 0.765 \text{ MeV}$ (-) | |
| $\text{T} + \text{T} \rightarrow 2\text{n} + ^4\text{He} + 11.327 \text{ MeV}$ (~1.259 MeV) | |
| $\text{T} + ^3\text{He} \rightarrow \text{n} + \text{p} + ^4\text{He} + 12.092 \text{ MeV}$ (~6.718 MeV) | |
| $\text{T} + ^3\text{He} \rightarrow \text{D} + ^4\text{He} + 14.319 \text{ MeV}$ (14.319 MeV) | |
| $^3\text{He} + ^3\text{He} \rightarrow 2\text{p} + ^4\text{He} + 12.861 \text{ MeV}$ (12.861 MeV) | |
| Proton-Based Fusion Fuels | |
| <u>Primary Reactions</u> | |
| $\text{p} + ^6\text{Li} \rightarrow ^3\text{He} + ^4\text{He} + 4.022 \text{ MeV}$ (4.022 MeV) | |
| $\text{p} + ^9\text{Be} \rightarrow ^4\text{He} + ^6\text{Li} + 2.125 \text{ MeV}$ (2.125 MeV) | |
| $\text{p} + ^9\text{Be} \rightarrow \text{D} + 2^4\text{He} + 0.652 \text{ MeV}$ (0.652 MeV) | |
| $\text{p} + ^{11}\text{B} \rightarrow 3^4\text{He} + 8.664 \text{ MeV}$ (8.664 MeV) | |
| <u>Secondary Reactions</u> | |
| $^3\text{He} + ^6\text{Li} \rightarrow \text{p} + 2^4\text{He} + 16.880 \text{ MeV}$ (16.880 MeV) | |
| $^3\text{He} + ^6\text{Li} \rightarrow \text{D} + ^7\text{Be} + 0.113 \text{ MeV}$ (0.113 MeV) | |
| $^3\text{He} + ^3\text{He} \rightarrow 2\text{p} + ^4\text{He} + 12.861 \text{ MeV}$ (12.861 MeV) | |
| $^4\text{He} + ^9\text{Be} \rightarrow \text{n} + ^{12}\text{C} + 5.702 \text{ MeV}$ (0.439 MeV) | |
| $^4\text{He} + ^9\text{Be} \rightarrow \text{n} + ^3\text{He} - 1.573 \text{ MeV}$ (-) | |
| $^4\text{He} + ^{11}\text{B} \rightarrow \text{p} + ^{14}\text{C} + 0.784 \text{ MeV}$ (0.784 MeV) | |
| $^4\text{He} + ^{11}\text{B} \rightarrow \text{n} + ^{14}\text{N} + 0.158 \text{ MeV}$ (0.011 MeV) | |
| $\text{p} + ^{10}\text{B} \rightarrow ^4\text{He} + ^7\text{Be} + 1.147 \text{ MeV}$ (1.147 MeV) | |

^aEnergy release is $Q(Q_+)$, where Q is total energy release including the energy of the neutron and Q_+ is the charged-particle energy only (p = protium, D = deuterium, T = tritium, n = neutron).

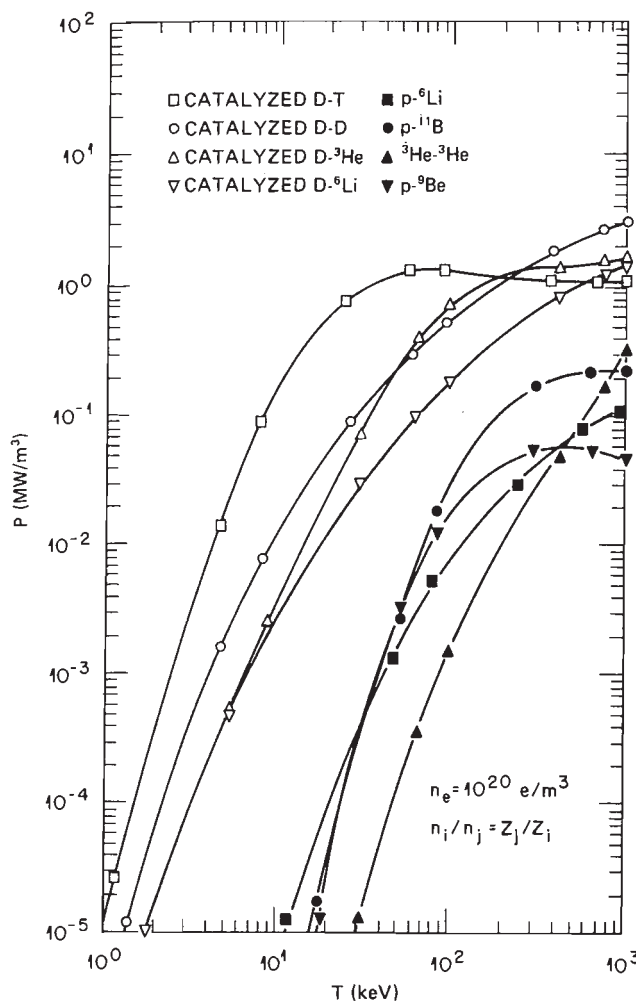


Fig. 1. Maximum charged-particle power release versus temperature for the principal fusion fuels in thermalized plasmas at $n_e = 10^{20} \text{ e/m}^3$ and $n_i/n_j = Z_j/Z_i$. Power output scales as the square of the electron density.

1. deuterium-tritium-lithium (D-T-Li) cycle⁷
2. D-D-T-³He or catalyzed D-D cycle^{7,8}
3. D-D-³He cycle⁷
4. D-⁶Li cycle⁹
5. p-¹¹B cycle.¹⁰⁻¹²

In the D-T-Li cycle, deuterium and lithium are the primary fuels. The lithium is required for tritium regeneration, which can be accomplished via neutron-induced reactions within a lithium-laden blanket surrounding the plasma.

The catalyzed D-D cycle uses only deuterium as the primary fuel. Unburned tritium and ³He generated by the D-D reactions are recycled into the

TABLE II
General Characteristics of Nuclear Fusion Fuels

"Classical" Fusion Fuel

D-T 20% charged particles, 80% 14 MeV n's.
Must breed tritium from lithium (D-T-Li reactor).
Radioactive tritium (~100 MCi).

"Conventional" Advanced Fusion Fuels

D-D } Practical advanced fusion fuels for steady-state,
D-⁶Li } moderate beta plasmas.
D-³He Relatively "clean" fuel burn. Dependent on n-T,
or D-D, or D-⁶Li economy.

"Exotic" Advanced Fusion Fuels

p-⁶Li } Need more study before acceptance as
p-⁹Be } "conventional" fusion fuels, i.e.,
p-¹¹B } $Q_P = \text{power out/power in} < 1$ at present

TABLE III
Fusion Fuel Costs*,†

| Fuel | Supplier ^a | Purity (%) | Cost (\$/kg) | Unit Fuel Cost (FBU = 1.0) ^b [mil/kW(thermal)·h] |
|-----------------|-----------------------|------------|---------------------|---|
| D | SRL | 99.1 | 1.063×10^3 | 0.008 |
| T | ML | (>94) | 7.5×10^6 | 42 |
| ³ He | ML | 99.9 | 7.35×10^5 | 4.5 |
| ⁶ Li | ORNL | 95 | 1.250×10^3 | 0.03 |
| ¹¹ B | EP | 97 | 3.6×10^4 | 1.7 |

*The U.S. Department of Energy established prices were provided by J. Ratledge and C. Benson (ORNL).

†Prices and purities subject to revision based on demand and technological improvements. (Tritium and ³He costs may be only a first-generation reactor cost.)

^aSRL = Savannah River Laboratory, ML = Mound Laboratory, ORNL = Oak Ridge National Laboratory, EP = Eagle-Picher Company.

^bFBU = fractional burnup = 1.0.

plasma such that the burnup rate of these fuels is equal to their production rate.⁸ Tritium regeneration in a blanket is not required. The fusion energy yield comes principally from the D-T, D-D, and D-³He reactions. In the D-D-³He cycle, deuterium is the primary fuel and the ³He generated by D-D reactions is recycled; however, the unburned tritium (~20 to 50%) is collected and stored for decay to ³He for use

as fuel, perhaps in a D-³He satellite reactor.¹³ Tritium regeneration is again not required. The fusion energy yield is mainly from D-³He and D-D reactions although a significant amount of tritium is burned.

The p-¹¹B cycle uses only naturally occurring isotopes and primarily produces ⁴He ash. There is no tritium as either fuel or reaction product to be handled. One weak side reaction produces ¹⁴C (see Table I), a long-lived radioactive nuclide that would require special control. Any ¹⁰B contamination of the ¹¹B fuel can generate radioactive ⁷Be via the p + ¹⁰B reaction (see Table I). The p-¹¹B reaction is the most reactive of the proton-based or exotic fuels, produces primarily charged particles, and is closest to satisfying ignition prospects at ion energies of about $T_i \approx 300$ keV. Other less reactive exotic fuels (e.g., p-⁹Be, p-⁶Li, and ³He-³He) are possible in principle but are less likely to satisfy ignition (and especially sustained burn) conditions unless new physics phenomena are discovered (e.g., very dense plasmas which confine gamma rays and bremsstrahlung analogous to neutron conservation in a fission reactor¹⁴).

The D-T-Li cycle can be identified as the classical fusion fuel cycle because of the extremely high reactivity parameter of D-T at low temperature (relative to the other fuels) and because of its relatively high fusion power density (Table I and Fig. 1). The fuel most likely to be used in first-generation reactors is D-T, and it seems likely that ignition of other fuels may require D-T ignition for startup followed by an adequate thermal excursion to permit transition to the advanced fuels.

PHYSICAL REQUIREMENTS FOR ATTAINING FUSION

Fusion fuel must be heated to a sufficiently high energy that the fast-moving fuel nuclei can overcome the Coulomb electrostatic repulsive forces between the electrically charged nuclei and then react. Because heating requires an investment of energy, the heated fuel must be confined (without escape to or contact with surrounding materials) long enough to allow more nuclear reaction energy (carried as the kinetic energy of neutrons and charged particles) to be released than is invested—referred to as energy break-even. It is likely that magnetically confined fusion plasmas must also be ignited or be very close to ignition to ensure a reasonable economic return. Driven, high Q_P (= power out/power in) machines may be economical even if unignited.

Ignition is the condition of a self-sustaining fusion reaction, requiring that the charged-particle energy release compensate for total plasma energy loss (particle and energy transport and radiation losses). Thus, the primary goal of scientific feasibility for fusion research is to achieve in the hydrogen plasma:

1. plasma energy T (keV)
2. electron density n_e (m^{-3})
3. plasma energy confinement time τ_E (s),

which together satisfy conditions for ignition. The simple product $(Tn_e\tau_E)_I$ for experimentally achieved plasmas is a useful and meaningful criterion for evaluating the degree of closeness to achieving the critical value of this product for ignition, $(Tn_e\tau_E)_I$. The same parameters in an experimental D-T plasma would then describe a self-sustaining D-T reaction. The $(Tn_e\tau_E)_I$ values for various fusion fuels are given in Fig. 2 and illustrate the marked advantage of D-T fuel over the other fuels—the lower the curve the more reactive the fuel.

Detailed ignition analysis should include other

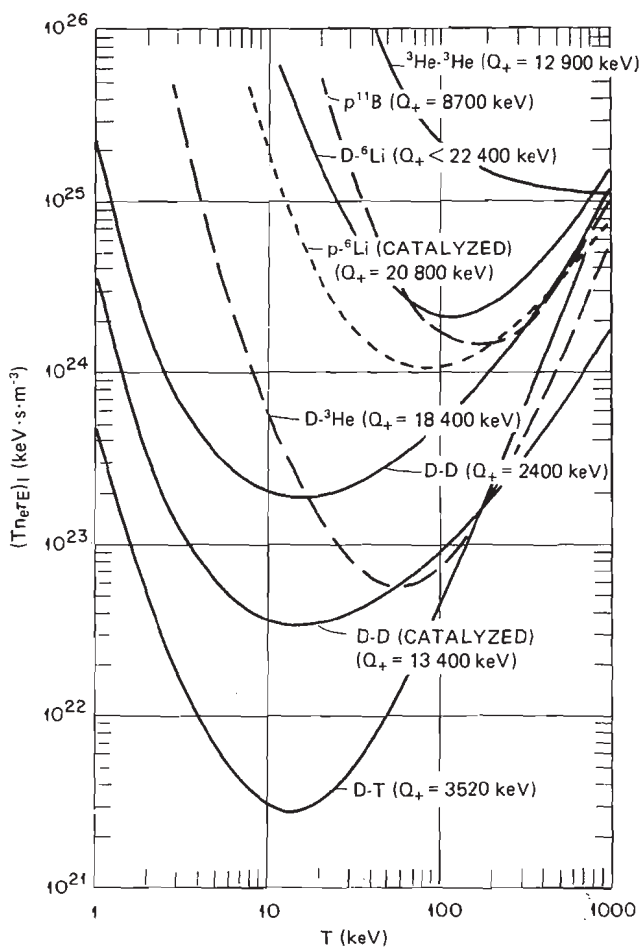


Fig. 2. Ignition curves $(Tn_e\tau_E)_I$ for various thermalized fuels as a function of ion temperature. Curves are for primary reaction only; thus, D-⁶Li does not include D-D and ⁶Li-⁶Li reactions, which would lower the D-⁶Li curve. Maximum power density occurs at curve minima since $(Tn_e\tau_E)_I \propto 1/\text{charged-particle power production}$.

factors such as fast fusion effects. By analogy with the fission multiplication constant, the four-factor plasma energy multiplication formula ($k \geq 1$ for ignition) is

$$k = f\eta\epsilon p ,$$

where

f = thermal energy utilization factor [$f = (T_{ne}\tau_E)_E / (T_{ne}\tau_E)_I$]

η = energy increment factor due to side reactions (e.g., D-D in a D-T plasma but $\eta \approx 1$ at 10 keV)

ϵ = fast fusion factor due to suprathermal particles (e.g., beam particles or knock-on fuel particles due to nuclear elastic or hard Coulomb collisions)

p = fusion product (FP) energy escape probability for loss of FP energy before *in situ* slowing down into the thermal region.^{15,16}

The k factor does not include profile or size effects and hence is analogous to the fission neutron accountability factor k_∞ .

Breakeven Criteria

The simplest expression for energy breakeven (when energy yield equals energy investment) of fusion reactions is given by

$$Q_P = \frac{\text{power output } (P_o)}{\text{power input } (P_i)} > 1 ,$$

where P_o stands for total plasma gain (including neutron energy) and P_i is the input power density to the plasma (including that to compensate radiation losses). For a pure hydrogenic plasma (e.g., D-T) with ion and electron energies $\frac{3}{2}T_i$ and $\frac{3}{2}T_e$, respectively, P_i is defined as

$$P_i = \frac{3}{2} \frac{n_e(T_i + T_e)}{\tau_E} \approx \frac{3n_e T}{\tau_E} ,$$

and the output power density P_o is

$$P_o = n_D n_T \langle \sigma v \rangle Q \leq \frac{1}{4} n_e^2 \langle \sigma v \rangle Q .$$

[For a fuel containing like nuclear reactants, P_o is $\frac{1}{2}(n_i^2 \langle \sigma v \rangle Q)$.] For energy breakeven in a 50:50 D-T fuel mix, this yields

$$(n_e \tau_E)_{En} \geq \frac{12T}{\langle \sigma v \rangle_{DT} Q} ,$$

where

n_e = electron density, e/m^3

τ_E = energy confinement time, s

$\langle \sigma v \rangle$ = reaction rate parameter for an assumed Maxwellian velocity distribution, m^3/s

Q = total fusion energy release of 17.586 MeV for D-T.

The minimum $(n_e \tau_E)_{En}$ is $\sim 6 \times 10^{19} m^{-3} \cdot s$ at $T \approx 10$ keV, and $(T_{ne}\tau_E)_{En}$ is then $\sim 6 \times 10^{20} \text{ keV} \cdot m^{-3} \cdot s$ for energy breakeven.

Lawson formulated a rather unique energy criterion, now known as the Lawson criterion.¹⁷ This criterion accounts for other limitations, apart from that of temperature, on the condition of operation of a fusion reactor. It considered a D-T (or D-D) system with pulse length t in which the input power to sustain the plasma losses [bremsstrahlung (P_B) and plasma energy throughput ($3nT/t$)] was less than the recovered power from total nuclear power release (P_N) plus the input power using a thermal recovery efficiency η of one-third. Thus,

$$P_B + \frac{3nT}{t} \leq \eta \left(P_N + P_B + \frac{3nT}{t} \right) .$$

Letting the pulse length t be the energy confinement time τ_E , one obtains

$$(n\tau_E)_L \geq \frac{24T}{\langle \sigma v \rangle_{DT} Q} \frac{1}{1 - 2P_B/P_N} .$$

In this expression, the basic limitation to ignition and burn of fusion plasmas is bremsstrahlung radiation in which electrons are accelerated in collisions with ions and other electrons and radiate as a result of the accelerated charge motion. This radiation loss term limits the minimum ignition temperature for D-T to ~ 4 to 5 keV and the maximum burn temperature to ~ 500 keV in an otherwise loss-less transparent plasma. At $T \approx 10$ keV, $P_B \ll P_N$ for a pure D-T plasma, and thus the Lawson criterion reduces to

$$(n\tau_E)_L \gtrsim \frac{24T}{\langle \sigma v \rangle_{DT} Q} ,$$

which is twice as difficult to achieve as the energy breakeven condition given above.

Ignition breakeven for D-T can be expressed as

$$(n_e \tau_E)_I = \frac{12T}{\langle \sigma v \rangle_{DT} Q_+} ,$$

where Q_+ is the charged-particle or alpha power only (3.517 MeV for D-T). (Only charged-particle power is used because only that power is available to sustain the plasma reaction; neutron power is carried out of the reaction chamber.) Because the ratio of total energy release to charged-particle power (Q/Q_+) is ~ 5 , ignition breakeven is five times more difficult to achieve than energy breakeven. This simple expression assumes *in situ* deposition of the D-T alpha energy and no profile effects, fast fusion effects, or impurities present.

The presence of impurities in the plasma will reduce the effective fuel density, and the appropriate three factor expression for D-T ignition becomes

$$(Tn_e\tau_E)_I \geq \frac{12T^2}{\langle\sigma v\rangle_{DT}Q_+} \cdot \frac{1 - \sum (Z_{imp} - 1)n_{imp}}{\left(1 - \frac{\sum Z_{imp}n_{imp}}{n_e}\right)^2},$$

where Z_{imp} is the effective charge of an impurity and n_{imp} its number density. Thus, if the plasma contains as much as 4% fully ionized oxygen (or 15% alpha ash) the ignition condition is almost twice as difficult to achieve as in a pure D-T plasma. Bremsstrahlung losses will also be more severe, but this is incorporated into the experimental $(\tau_E)_E$ [i.e., the total energy containment time defined by $1/(\tau_E)_E = \sum 1/\tau_{loss}$, where the sum is taken over all plasma thermal energy loss processes].

Figure 2 illustrates the ignition parameter $(Tn_e\tau_E)_I$ for several proposed fusion fuels and shows the increasing degree of difficulty of igniting the advanced fusion fuels. Because $(Tn_e\tau_E)_I \propto T^2/\langle\sigma v\rangle \propto \beta^2 B^4/P_{fusion}$, in the case of constant plasma pressure and constant B the curves are inversely proportional to the fusion power density, and D-T is the most reactive of all fuels up to ~ 150 keV (Ref. 16). Here, β is the ratio of the total plasma pressure (ΣnT in $J \cdot m^{-3}$) to magnetic pressure ($B^2/2\mu_0$) and is a measure

of the efficiency of using the applied magnetic field B (in Tesla). The permeability $\mu_0 = 4\pi \times 10^{-7} H/m$.

Ignition and Burning Temperature

Ignition is the major scientific feasibility goal (after energy break-even) of fusion research; however, the ignition point represents a condition of unstable equilibrium (positive temperature coefficient). Thus, the temperature of an ignited magnetically confined plasma^a will increase (in several seconds) to the operating or burning temperature, which represents a stable operating point characterized by a negative temperature coefficient, if the fuel and ash mix does not change. Associated with the burning or operating temperature is a positive density coefficient (i.e., increase of the fuel/ash ratio increases the fusion power and vice versa).

The negative temperature property of the operating temperature can be visualized by consideration of Fig. 3. An increase (decrease) in ion temperature of plasma resulting from a temperature perturbation decreases (increases) the fusion to radiation power ratio, causing the plasma to hunt about the operating

^aThe term "burning plasma" refers to conditions where the fusion energy exceeds the driver energy supplied to sustain the plasma. An "ignited" plasma is one in which fusion reactions proceed without external energy being supplied.

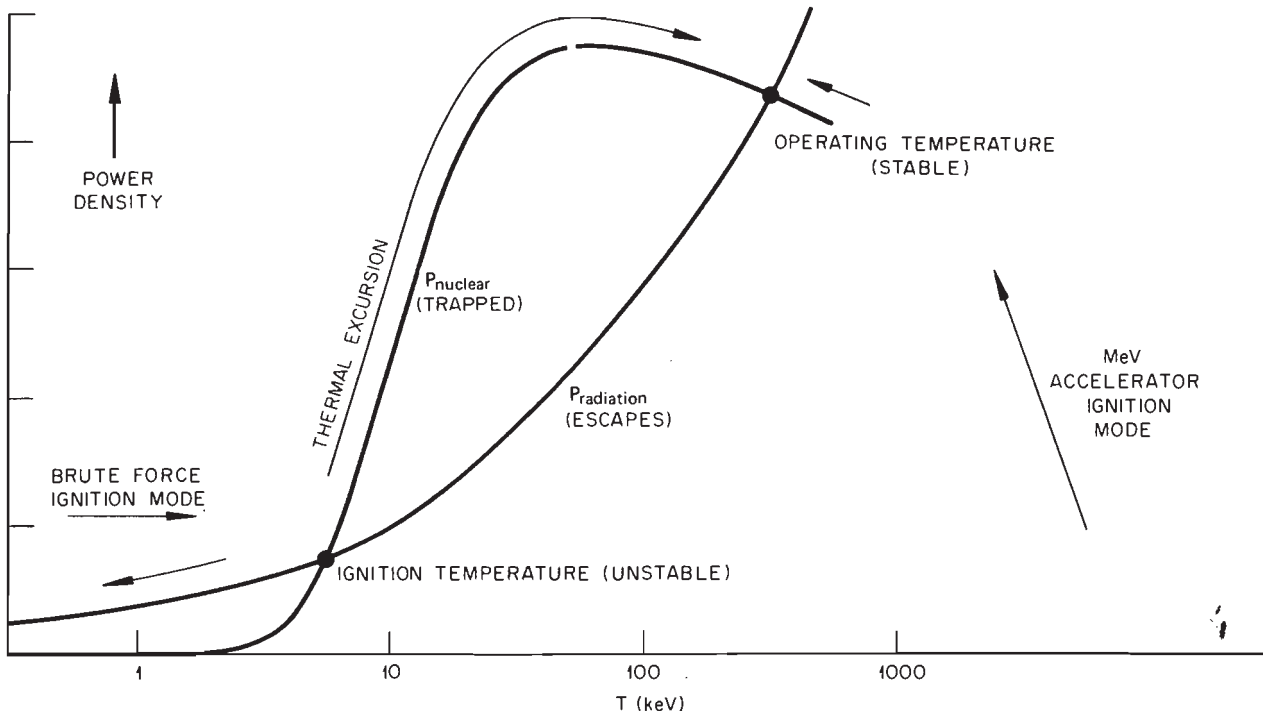


Fig. 3. Schema of D-T plasma burn characteristics versus ion kinetic temperature: $P_{nuclear}$ = nuclear power deposited in plasma; $P_{radiation}$ = radiation power loss from plasma. Other losses would lower the operating temperature.

temperature for the case of constant fuel/ash mix. Losses in addition to bremsstrahlung and synchrotron radiation (e.g., conduction, convection, and diffusion of particles and energy, as well as instabilities) will shift the operating temperature down from that limited by radiation alone.

The desired operating temperature is sometimes selected as that point at which the power density is maximum, i.e., where $\langle\sigma v\rangle/T^2$ is a maximum, which occurs at about 15 keV for pure D-T (minimum in Fig. 2). With the possible exception of severe loss modes, it is unlikely that a steady-state burning plasma would be limited to such low temperatures since even ash buildup would require somewhat higher operating temperatures for steady-state burns. Operating too near the maximum power density point may lead to severe wall loading problems, and the plasma may become more susceptible to instability quenching. However, such reactor operation can lead to a smaller reactor system.

Approach to Ignition

Plasmas may be generated by various heating and formation processes, but generally they involve

1. ohmic or resistive heating
2. injection and trapping of energetic particles
3. radiofrequency (rf) heating (electron cyclotron, ion cyclotron, or hybrid heating techniques).

Tokamak plasmas are initiated by ohmic heating generated by inductively producing a high toroidal current through the gas to break it down into ions and electrons (i.e., a plasma) and then resistively heating the plasma; however, this approach has been limited in present experiments to temperatures of less than ~1 keV. The STARFIRE tokamak reactor may be ignited by rf drive of the plasma current.^{3,18} Adding neutral beam heating (e.g., >2 MW in the PLT) has permitted the achievement of ion temperatures T_i up to 7.1 keV with powerful neutral beam heating supplementing the ohmic heating.¹⁹

The 2XII-B [now Beta II—a Yin-Yang^b mirror facility at Lawrence Livermore National Laboratory (LLNL)] achieved $T_i \approx 10$ keV (but $T_e \lesssim 200$ eV) with massive energetic neutral beam injection.²⁰ This low electron temperature poses a problem on the attainable $T_{n\tau}$ value because the slowing down of hot ions permits an $n\tau$ value of only

$$n_e \tau_{ie} \approx 5 \times 10^{17} T_e^{3/2} \frac{T_i}{(T_i - T_e)} (\text{m}^{-3} \cdot \text{s}) ,$$

where T is in keV and τ_{ie} is the ion slowing down time on the cooler electrons. Thus, this plasma is

limited to $\sim 5 \times 10^{16} \text{ m}^{-3} \cdot \text{s}$ unless electron cyclotron resonance heating of the electrons could be provided. The new Tandem Mirror Experiment (TMX) at LLNL has achieved $n\tau \approx 10^{17} \text{ m}^{-3} \cdot \text{s}$ in the central cell but at low temperatures.²¹ Electron cyclotron resonance heating is planned for the upgraded TMX and future mirror experiments [e.g., the Mirror Fusion Test Facility (MFTF), a larger Yin-Yang device] as well as MFTF-B, which will be a large TMX (basically two Yin-Yang coil configurations separated by a long solenoidal section) at LLNL.

Figure 4 compares several experimentally achieved values of $T_{n_e \tau_E}$ with the D-T ignition curve at the same kinetic temperature. Also shown are the energy breakeven criterion and the Lawson criterion (expressed as $T_{n\tau}$) for D-T. The bremsstrahlung limit for a hydrogenic plasma and the open mirror loss curves for a deuterium plasma in a 2:1 magnetic mirror are also presented. Ignition cannot occur above these two loss curves; hence, reduction of mirror end losses is essential to achieve ignition in open mirror devices.

Representative values of the thermal energy utilization factor, f [the ratio of $(T_{n_e \tau_E})_E$ to $(T_{n_e \tau_E})_I$], are presented in Fig. 5 as a function of year for several different experiments. Note that toroidal devices have shown improved plasma quality by 1000 fold every 10 years since 1958 (see Fig. 5).

Energy breakeven is closer to achievement than ignition by a factor of 5, whereas in beam-driven plasmas one may gain another factor of ~3 because of the fast fusion effect.¹⁶ This would place PLT within a factor of ~40 from energy breakeven, neglecting profile effects (see also Grisham,²² who estimates about a factor of 44). The Massachusetts Institute of Technology Alcator tokamak has not achieved reactor-relevant ion temperatures as yet but has achieved $n\tau \approx 3 \times 10^{19} \text{ m}^{-3} \cdot \text{s}$. The Frascati Tokamak (FT) has apparently reached $4 \times 10^{19} \text{ m}^{-3} \cdot \text{s}$ at $T = 1.3$ keV and a $T_{n\tau}$ index value about twice that of Alcator²³; however, because of the higher temperature the FT device has a tenfold improvement in the value of f compared to Alcator.

In the hot ion ignition mode,^{24,25} external heating (e.g., by beams and/or by rf heating) drives $T_i > T_e$ —this relaxes the ignition conditions further. It is possible that the next generation of plasma experiments may demonstrate ignition in the mainline magnetic confinement approaches [e.g., the Tokamak Fusion Test Reactor (TFTR), the Joint European Torus Tokamak, MFTF-B, etc.].

Approaches to Fusion Power

To extract useful energy from nuclear fusion, the reactor must confine the plasma at fusion temperature for a sufficient time for the reaction to occur

^bTwo magnet coils shaped like the outline of cupped hands.

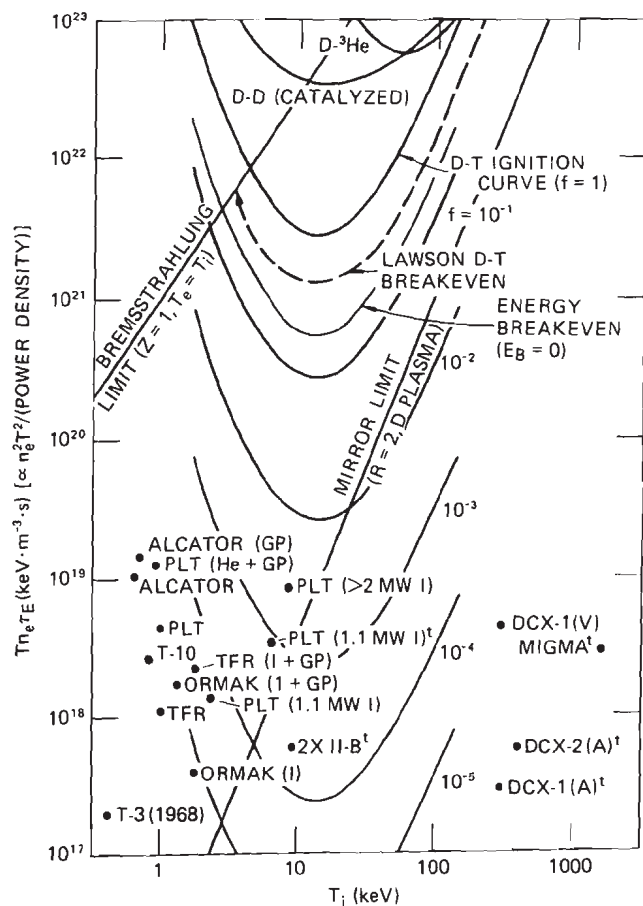


Fig. 4. Three-factor formula ($Tn_e \tau_E$) plot versus T_i of several magnetic confinement experimental points, the ignition curves for three fuels, the Lawson breakeven curve, the energy break-even curve ($E_B = 0$), and the limiting bremsstrahlung and mirror (2/1 mirror) loss curves for D-D plasma; I = neutral beam injection; GP = gas puff.

with a significant gain as measured by Q_P . Two fundamentally different approaches are now being followed for plasma confinement:

1. magnetic confinement
2. inertial confinement.

For magnetic confinement, the expanding plasma is contained in carefully shaped magnetic fields; the kinetic pressure of the plasma is restrained by magnetic field pressure, which may be due in part to plasma currents. Plasma heating can be provided by the magnetic field system (resistive heating from induced plasma currents) and/or by an auxiliary system (e.g., electromagnetic wave or beam drivers). Reactors based on magnetic confinement would typically operate with densities ranging from $\sim 10^{21}$

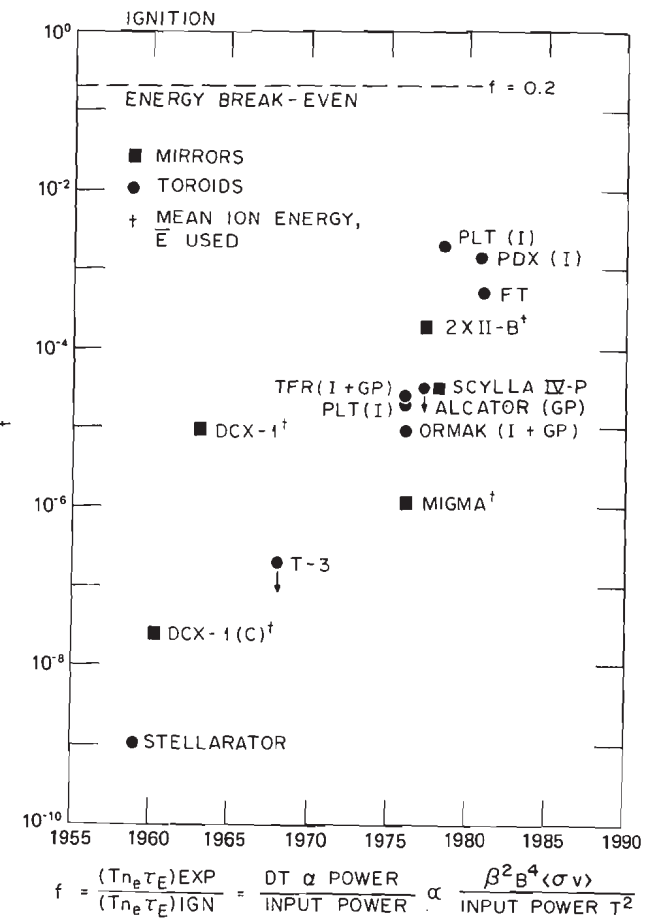


Fig. 5. Progress in magnetic mirror and toroidal confinement versus year: f = thermal energy utilization factor (Ref. 16), C = carbon arc dissociation, and t = non-thermal.

down to 10^{19} particle/m³ to minimize plasma-exerted pressure at fusion temperatures (10 keV or higher). For ignition of D-T fuel at 10 keV, the required value of the product of particle density and confinement time ($n_e \tau_E$) is 3×10^{20} m⁻³·s, and, hence, the associated energy confinement times (τ_E) would range from ~ 0.3 to 30 s. The Fusion Engineering Device is the most advanced tokamak engineering design in planning²⁶ (International Tokamak Reactor on the international level) whereas STARFIRE is the most advanced tokamak reactor design.^{3,18}

The objective of inertial confinement is to heat small fuel pellets to fusion ignition conditions by using powerful, fast-pulsed energy beam drivers such as laser, electron, or ion beams. Ablation of the surface layer of the pellet by the energy beam results in compressional heating of the core of the pellet. Confinement is achieved if the heating process is rapid enough for a significant fraction of the hot, compressed plasma to burn before thermal disassembly of the pellet terminates the reaction. Pellets must

be restricted in size (~ 5 mm or less in radius) to prevent the microexplosion (~ 100 MJ) on ignition from seriously damaging the containing vessel. Present plans call for attaining repetitive pellet burns somewhat analogous to a combustion chamber of a giant automobile engine, but with a cycle rate of 10 to 50 s^{-1} . For inertial confinement, the same ignition condition applies, but it is usually expressed as ρr , where ρ is the density in kg/m^3 and $r = v_s \tau_I$ and where the sound velocity is $v_s = [5\Sigma(nT)/3\rho]^{1/2} = 1.13 \times 10^6 \text{ m/s}$ for D-T at 10 keV. Thus, for D-T (uncompressed solid density = 213 kg/m^3), ignition requires

$$\rho r = \rho v_s \tau_I \approx 1.4 \text{ kg/m}^2 ,$$

and required confinement times for ignition, τ_I , are in the nanosecond range. Reactors based on inertial confinement would operate with pellet compression densities of $\sim 1400 \text{ kg/m}^3$ or more and compressed radii of ~ 1 mm or less.

Tritium Burnup

Recirculation of unburned tritium is a major problem of deuterium-based fusion reactors. The tritium source feed rate S_T equals the burnup rate plus the throughput rate, i.e.,

$$S_T = \frac{n_T}{\tau_T} + n_D n_T \langle \sigma v \rangle_{DT} ,$$

giving for the fractional burnup of tritium (FBT)

$$FBT = \frac{n_D n_T \langle \sigma v \rangle_{DT}}{S_T} \approx \frac{n_D \tau_T \langle \sigma v \rangle_{DT}}{1 + n_D \tau_T \langle \sigma v \rangle_{DT}} ,$$

neglecting non-D-T reactions (which are generally much less frequent).

Table IV tabulates the expected burnup of tritium as a function of $n_D \tau_T$ and ion temperature. Here, n_D is the deuteron density in m^{-3} and τ_T is the triton containment time. If one wishes to reduce the recirculation of tritium, the need for high temperature burns at large $n\tau$ values is obvious. In D-D reactors at high temperatures one may obtain burnup fractions of ~ 0.5 to 0.8 since n_D is appropriately higher than in D-T systems. One has potentially conflicting requirements, i.e., high temperatures to maximize tritium burnup and modest temperatures to optimize power density ($\langle \sigma v \rangle/T^2$).

An additional source of tritium burnup occurs in plasmas which produce energetic protons. The elements of a propagation chain reaction exist in a plasma containing deuterium, tritium, and ^3He , i.e.,



About 10% of the 14-MeV protons may be consumed as they slow down, with the product neutron being much less energetic than that from the one-step D-T

TABLE IV
Tritium Burnup

| $n_D \tau_T^a$ ($\text{m}^{-3}\cdot\text{s}$) | T (keV) = | | |
|--|--|------------------------|------------------------|
| | 10 | 25 | 50 |
| | $\langle \sigma v \rangle_{DT}$ ($\text{m}^3\cdot\text{s}^{-1}$) = | | |
| 3×10^{20} | 1.13×10^{-22} | 5.63×10^{-22} | 8.54×10^{-22} |
| 6×10^{20} | 0.03 | 0.14 | 0.20 |
| 10×10^{20} | 0.06 | 0.25 | 0.34 |
| 10×10^{20} | 0.10 | 0.36 | 0.46 |

^aFor a 50:50 pure D-T mixture $n_e \tau_T = 2n_D \tau_T$.

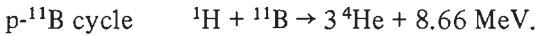
reaction. For thermalized protons at $T_i = 200$ keV, the rate parameter for $p + T$ is quite large ($\langle \sigma v \rangle = 1.52 \times 10^{-23} \text{ m}^3/\text{s}$).

D-T-Li FUEL CYCLE VERSUS ADVANCED FUEL CYCLES

Emphasis in the U.S. Department of Energy fusion energy program (and internationally) is on the D-T-Li fuel cycle, with only modest effort devoted to pursuing reactor prospects of advanced fusion fuel cycles. However, in the long range some advanced reactor fuel may be more desirable than D-T. Regardless of whether or not the ultimate potential of fusion lies with an advanced fuel cycle, planned experimental reactors and early-generation demonstration reactors will probably use the D-T-Li fuel cycle.

Four fuel cycles and possibly the $p-^{11}\text{B}$ cycle offer potential for extrapolation to power-producing fusion reactors. These cycles and the primary reactions are

| | |
|-----------------------|--|
| D-T-Li cycle | $^2\text{D} + ^3\text{T} \rightarrow ^4\text{He} + n + 17.6 \text{ MeV}$ |
| D-D cycle | $\begin{cases} ^2\text{D} + ^2\text{D} \rightarrow ^1\text{H} + ^3\text{T} + 4.03 \text{ MeV} \\ ^2\text{D} + ^2\text{D} \rightarrow ^3\text{He} + n + 3.27 \text{ MeV} \end{cases}$ |
| $D-^3\text{He}$ cycle | $^2\text{D} + ^3\text{He} \rightarrow ^1\text{H} + ^4\text{He} + 18.3 \text{ MeV}$ |
| $D-^6\text{Li}$ cycle | $^2\text{D} + ^6\text{Li} \rightarrow 5$ exothermic reactions (see Table I) |



Whereas other reactions were also listed in Table I, the first four fuels have much higher reactivity and are judged the most likely to be viable fusion fuels (see Fig. 1).

D-T Fuel

The D-T fuel is projected for use in all fusion ignition experiments and in first-generation reactors

because of its extremely high ignition potential at the lowest temperature. It is thus the reference fusion fuel and has been specified in almost all reactor design studies. The time scale for the advent of advanced fuel reactors is unknown and may require further physics development, although preliminary studies of very large tokamaks burning in a catalyzed D-D mode look promising.

Concern for the environmental impacts of D-T-fueled reactors is based on the radioactive nature of the primary fuel constituent (tritium: 12.3-yr half-life; β up to 18 keV), the copious activation and radiation damage of materials by 14-MeV neutrons, and the absolute requirement for breeding tritium fuel in a lithium-rich blanket region located external to the burning plasma. Up to several hundred tons of lithium may be needed in the blanket of a D-T-Li tokamak reactor.

Even advanced fuel cycle reactors may require startup scenarios involving the use of small amounts of D-T fuel for ignition, followed by thermal excursion to elevated burning temperatures (Fig. 3), when less reactive but perhaps more environmentally and economically acceptable fuels may be used (provided the improved plasma quality needed to attain their ignition $T_{n\tau_E}$ can be achieved).

The D-T reaction delivers 80% of its power in the 14-MeV neutron and 20% in the charged alpha particle. In addition, the neutron will generate from ~2 to 4.8 MeV by exothermic reactions in the lithium blanket (see Table V). Thus, because there is no method other than the thermal conversion method for transforming the total neutron energy release (85 to 90% of total) to electricity, the D-T-Li cycle will be restricted to the 30 to 40% recovery efficiency of a thermal conversion cycle. Also, a significant fraction of the alpha energy will be converted to electromagnetic radiation, deposited at the first wall, and transferred to the thermal recovery system.

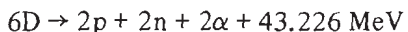
The unique environmental concerns in D-T-Li reactors, compared to other thermal power sources, are the large tritium inventory in the plant (about 2 to 40 kg corresponding to 20 to 400 million Ci activity) and in the plasma (~1 g), the lithium requirements (~50 to 1000 tons per reactor), the

increased complexity of heat exchangers, and the greater potential for 14-MeV neutron activation of the structural components surrounding the plasma. Depleted tritium D-T burns offer a reduced need for high tritium breeding ratios and offer a gradual transition to the catalyzed D-D reactor (Table VI).

The advanced fuel reactors can best be discussed relative to the D-T reference fuel. Table VII gives a comparison of the three main candidate fuels to D-T, in terms of those characteristics that are expected to influence the environmental impact of fusion. Each of these three advanced fuels is discussed below.

D-D Fuel

Advanced fuels lend themselves to direct electrical recovery of a larger fraction of the fusion power because charged-particle energy constitutes >50% of the released energy. The catalyzed D-D cycle is characterized by recycling of unburned tritium and ^3He produced in first generation D-D reactions such that the tritium and ^3He burnup ratios are equal to their production rates.⁸ Consider the fully catalyzed D-D reaction, which can be written as



$$(Q_+ = 26.707 \text{ MeV}),$$

with 61.8% of energy released in charged particles. The two neutrons will provide additional thermal energy release, but because tritium does not have to be manufactured by these neutrons, their additional output on capture after thermalizing can be made modest by using hydrogen (e.g., $n + \text{H} \rightarrow \text{D} + 2.226 \text{ MeV}$), large by using sodium ($n + \text{Na} \rightarrow \text{Mg} + e + 12.480 \text{ MeV}$), or very large by using fissile materials (~200 to 1000 MeV/n in converter fission reactors). Of the 61.8% charged-particle energy release, about one-half ends up as radiation deposited on the first wall, which must be recovered by thermal conversion, leaving ~31% for possible direct electrical conversion. Each 1% of direct conversion power gain is worth about three times the value obtainable by thermal conversion because of conversion efficiency. This is a critical factor in the efficiency of any power plant—it also decreases the waste heat and thus reduces the environmental impact.

Catalyzed D-D fusion requires isotopic separation of unburned tritium and ^3He from other ashes (e.g., protium and ^4He). The tritium and ^3He plus deuterium fuel makeup is used to refuel the reactor. The lower concentration and lower throughput of tritium and its higher burnup in the catalyzed D-D-fueled system are important environmental factors favoring its use over the D-T-Li system. Furthermore, elimination of the tritium breeding blanket would reduce the gross inventory of tritium by a factor of >100, and the activation of structural material would be reduced

TABLE V

Principal Neutron Reactions with Lithium

| |
|---|
| $n_{\text{thermal}} + ^6\text{Li} \rightarrow \text{T} + ^4\text{He} + 4.784 \text{ MeV}$ |
| $n_{\text{fast}} + ^6\text{Li} \rightarrow n' + \text{D} + ^4\text{He} - 1.474 \text{ MeV}$ |
| $n_{\text{fast}} + ^7\text{Li} \rightarrow n' + \text{T} + ^4\text{He} - 2.467 \text{ MeV}$ |
| $n_{\text{fast}} + ^7\text{Li} \rightarrow n' + ^7\text{Li}^* - 0.478 \text{ MeV}$ |
| $\rightarrow n' + ^7\text{Li} + h\nu - 0.478 \text{ MeV}$ |

TABLE VI
Tritium Production in D-T Reactors with Depleted Tritium

| Operating Temperature (keV) | Tritium Produced/Tritium Consumed ^a | | | Required Tritium Breeding Ratios |
|-----------------------------|--|--|---|----------------------------------|
| | (n _T /n _D = 1) (%) | (n _T /n _D = 0.1) (%) | (n _T /n _D = 0.02) (%) | |
| 30 | 0.36 | 3.6 | 18 | 1.00/0.96/0.82 |
| 60 | 0.71 | 7.1 | 36 | 0.99/0.93/0.64 |
| 90 | 1.2 | 12 | 60 | 0.99/0.88/0.40 |
| 120 | 1.7 | 17 | 85 | 0.98/0.83/0.15 |
| 150 | 2.3 | 23 | 115 | 0.98/0.77/0.00 |
| 180 | 3.0 | 30 | 150 | 0.97/0.70/0.00 |

^aTritium produced $\approx \frac{1}{2} n_D^2 \langle \sigma v \rangle_{DDT}$. Tritium consumed $\approx n_D n_T \langle \sigma v \rangle_{DT}$. Tritium produced/tritium consumed $\approx n_D \langle \sigma v \rangle_{DDT} / 2n_T \langle \sigma v \rangle_{DT}$.

TABLE VII
Comparison of the Characteristics of D-T and Principal Advanced Fusion Fuels

| Characteristic | D-T | D-D | Lean D- ³ He | D- ⁶ Li |
|--|-----------------|-------------------------|--|--------------------------|
| Energy yield per reaction pair, MeV | 17.6 | 3.65 | 18.3 | Up to 22.4 |
| Fraction energy carried by neutrons, % | 80 | ~35 | ~2 | <35 |
| Neutron energy, MeV | 14.1 | 2.45(14.1) ^a | 2.45(14.1) ^a | ~2.0(14.1) ^a |
| Ratio of activation in structure, % | 100 | 20 to 60 | <2 | <20 to 60 |
| Radioactive fuel or ash | Tritium | Tritium | Tritium | Tritium, ⁷ Be |
| Percent tritium fuel, % | 50 | <3 | <1 | <3 |
| Inventory of tritium, kg | ~10 | <0.001 | <0.001 | <0.001 |
| Special fuel cycle required ^b | Lithium blanket | None | Production fusion reactors for ³ He | None |

^aContributions from D-D (or D-D and D-⁶Li) and D-T side reactions.

^bIsotope separation is required in all cases.

by a factor of 2 since only ~45% of the neutrons are of 14-MeV energy.

Table VIII summarizes the advantages and disadvantages of the catalyzed D-D reactor. Saltmarsh et al.²⁷ have pointed out the improved breeding prospects for the catalyzed D-D systems over D-T. Overall one concludes that a catalyzed D-D reactor appears to offer the highest potential for fusion.

D-³He Fuel

A relatively "clean" (lean-deuterium, rich-³He) sequence can achieve²⁸ a gross reduction in neutron power output to $P_n \lesssim 2\% P_{total}$; however, ³He fueling depends on D-T-Li or partially catalyzed D-D reactors for ³He production (tritium decays to ³He with a 12.3-yr half-life). Using ³He production reactors on

reservation sites with satellite D-³He reactors near load sites has been proposed.¹³ In the D-³He reactions perhaps only ~50% of the total charged-particle energy release is subject to direct conversion prospects due to radiation and high particle transport to the walls.

Little tritium and few neutrons are produced in this fuel cycle, yielding a low inventory of radioactivity in the fuel system and a reduced level of activation in reactor structures.

D-⁶Li Fuel

The D-⁶Li fuel cycle is extremely complicated, having two D-D branches, five D-⁶Li branches, and six ⁶Li-⁶Li branches, all of which are exothermic. After about two generations there are more than 80

TABLE VIII
Advantages and Disadvantages of Catalyzed
D-D-Fueled Reactors

| |
|--|
| Advantages |
| 1. Lowest fuel cost; gaseous fuel and ashes. |
| 2. Modest total tritium inventory (~ 1 g); no lithium blanket. |
| 3. Optimal selection of primary heat exchanger and structures. |
| 4. Fissile and ^3He fuel breeding prospects. |
| 5. About 45% as many 14-MeV neutrons as D-T case. |
| 6. Steady-state burn prospect. |
| 7. Higher tritium burnup fraction than D-T case. |
| Disadvantages |
| 1. Rapid isotopic separation and fuel makeup required. |
| 2. Total neutron flux comparable to D-T. |
| 3. Requires higher temperatures and nT 's than D-T. |
| 4. Requires $\beta > 15\%$ for economic burn. |
| 5. Major safeguards problem (neutrons are "free"). |

exothermic (plus some endothermic) reactions that should be followed. There are two slight advantages of D- ^6Li over D-D reactors:

1. Li^{3+} will charge exchange rapidly with any neutral deuterium or tritium that is formed and thus keep the ionization level high
2. the lithium (and other high Z nuclei) cool the reaction down (via increased radiation losses), thus increasing the power density through $\langle \sigma v \rangle / T^2$.

It is, however, less reactive than D-T, D-D, and D- ^3He (see Fig. 1). Steady-state burns have been obtained with equilibrium ash present for $n_{^6\text{Li}}/n_D \lesssim Z_D/Z_{^6\text{Li}} = 0.33$.

The condensable property of the high Z isotopes may pose a severe solid ash problem in high vacuum systems although there will perhaps be a smaller amount of sputtered materials produced in any magnetic fusion reactor. The problem of condensable, unburned fuels as well as ashes (e.g., ^6Li , ^7Li , ^7Be , ^9Be , ^{11}B , etc.) in high vacuum systems may be a more onerous problem than that of first wall sputtering. Thus, the assumption of solid fuel burnup in the range of, say, 30% per pass will lead to ~ 1 to 2 tons per GW(thermal)-yr of unburned (lithium, beryllium, or boron) fuel deposited on colder surfaces of the vacuum chamber.

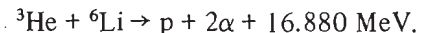
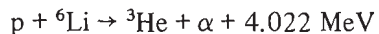
Exotic Fuel Cycles

The exotic fuels include $^3\text{He}-^3\text{He}$ and the proton-based fusion fuels: p- ^6Li , p- ^9Be , and p- ^{11}B . As shown in Fig. 2, these fuels are significantly less reactive than the classical fuel D-T or conventional advanced

fusion fuels (D-D, D- ^3He , or D- ^6Li). Low output power and adverse neutron production for p- ^9Be make this exotic fuel unsatisfactory as a "clean" economic and advanced fusion fuel.

The p- ^{11}B fuel cycle is the only proton-based fuel cycle with adequate reactivity for serious consideration here. Condensable and radioactive ash deposition could introduce both technological and radiological problems in the vacuum systems. Neutron production is lowest in this fuel cycle of the four fuel cycles considered. Some radioactive ^7Be is produced in the p- ^{10}B reaction should the ^{11}B not be isotopically pure. No steady-state burn has yet been projected for p- ^{11}B , although ignition prospects appear good for bremsstrahlung losses and alpha removal only.¹²

The fuel p- ^6Li has an important second-generation reaction that contributes to the following propagation chain reaction feature²⁹:



If the second reaction occurs while the suprathermal ^3He nucleus slows down in the plasma, the total energy production is 20.902 MeV, thus elevating the p- ^6Li curve of Fig. 2 by a factor of slightly more than 5. The fast proton might then trigger another cycle of reactions. However, in an actual plasma situation this reaction can occur only 10 to 20% of the time for various proton source energies and possible electron temperatures up to 300 keV. It is further complicated by the competing dissociation reaction $\text{p} + ^6\text{Li} \rightarrow \text{p}' + ^6\text{Li}^* - 2.2 \text{ MeV} \rightarrow \text{p}' + \text{D} + ^4\text{He} - 1.5 \text{ MeV}$. Figure 6 illustrates reaction rate parameters and fast fusion probabilities for energetic protons slowing down in a lithium plasma at various T_e .

It should be noted that the p- ^6Li fuel produces copious neutrons and radioactive ^7Be via the $^6\text{Li} + ^6\text{Li} \rightarrow \text{n} + ^4\text{He} + ^7\text{Be} + 1.908 \text{ MeV}$ reaction channel, a point first made by Ruby and Lung.³⁰ Also, neutron-rich deuterium nuclei and radioactive ^7Be are generated via the important $^3\text{He} + ^6\text{Li} \rightarrow \text{D} + ^7\text{Be} + 0.113 \text{ MeV}$ reaction channel.³¹ No steady-state burn prospects for p- ^6Li have yet been demonstrated.

The $^3\text{He}-^3\text{He}$ reaction should be studied further because nuclear elastic collisional promotion of ^3He ions into the suprathermal region, resulting from collisions with energetic protons and alpha particles, should improve reaction prospects for this fuel. It has other desirable features such as noncondensable fuel and ashes and no prospects for direct production of neutrons, deuterium, or tritium below the center of mass energy thresholds of 7.720, 5.493, or 6.954 MeV, respectively. There is a small gamma production cross section for $^3\text{He}-^3\text{He}$ reactions that rises from $0.4 \times 10^{-34} \text{ m}^2$ at $E_{^3\text{He}} = 0.86 \text{ MeV}$ to $9.2 \times 10^{-34} \text{ m}^2$ at 11.8 MeV (Ref. 32). Availability of ^3He as fusior

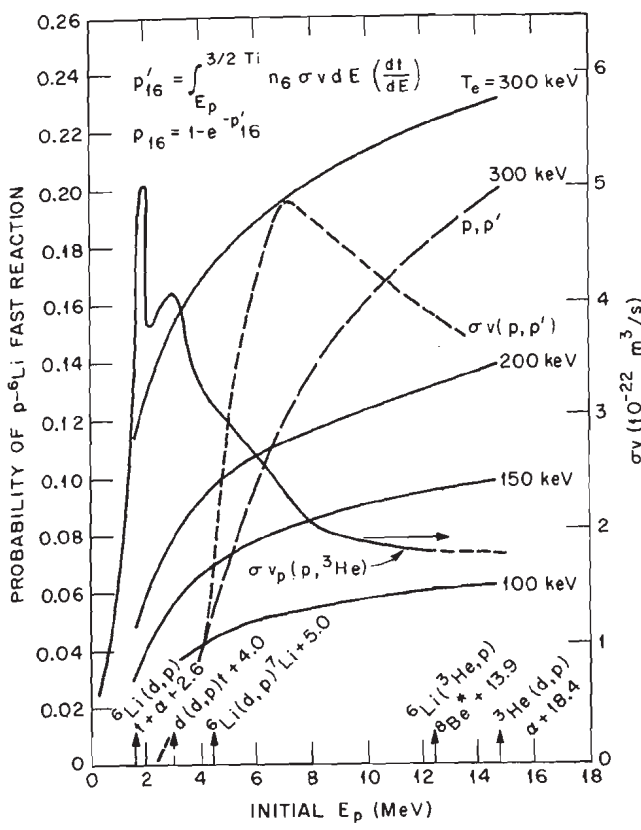


Fig. 6. Fast proton reactions with ${}^6\text{Li}$ in high temperature reactors: $\sigma v_p(p, {}^3\text{He})$ is σv for $p + {}^6\text{Li} \rightarrow {}^3\text{He} + \alpha + 4.0$ MeV; $\sigma v(p, p')$ is σv for $p + {}^6\text{Li} \rightarrow p' + {}^6\text{Li}^* - 2.2$ MeV $\rightarrow p' + d + \alpha - 1.7$ MeV. Fast fusion reaction probability curves are shown for several electron temperatures [solid lines are for $(p, {}^3\text{He})$ and dashed lines for (p, p')]. Electron temperatures will probably not exceed 150 keV in realistic plasmas which are magnetically confined.

fuel poses a serious problem because it does not occur naturally in significant concentrations; therefore, its origin for an "ultraclean" fusion reactor would depend on partially catalyzed D-D reactors from which excess ${}^3\text{He}$ and tritium (which decays to ${}^3\text{He}$) were separated and stored for eventual ${}^3\text{He}$ shipment to a ${}^3\text{He}-{}^3\text{He}$ reactor, if such a reactor proves feasible.

RADIATION LOSSES

There are three main types of electromagnetic radiation losses to be expected in burning plasmas:

1. spectrum line radiation due to incompletely ionized impurities
2. x-ray radiation due principally to bremsstrahlung radiation
3. cyclotron (or synchrotron) radiation losses.

Most estimates of ignition criteria demand only that the charged-particle fusion power production exceed the bremsstrahlung power loss, but in realistic situations impurity radiation and recombination [$X^{i+} + e \rightarrow X^{(i-1)+} + h\nu$] radiation play a major role in present-day plasmas. High temperature burning plasmas in the reactor regimes will be dominated by bremsstrahlung and synchrotron radiation (in a well-reflected situation the synchrotron radiation usually exceeds the bremsstrahlung above about $T_e = 15$ keV).

Bremsstrahlung Radiation

Bremsstrahlung (or braking) radiation in fusion plasmas is due to collisions between a Maxwellian sea of electrons with ions of charge Z_i and is usually expressed for low temperatures as^{33,34}

$$P_{Bei} = 3.033 \times 10^{-21} \bar{g}_{ff} n_e n_i Z_i^2 \sqrt{T_e} \quad (\text{keV/m}^3 \cdot \text{s}),$$

with n in m^{-3} (e = electron, i = ion), T_e in keV, and $\bar{g}_{ff} = 2\sqrt{3}/\pi = 1.103$ in the Born approximation. The radiation spectrum has more than 50% of the radiation power concentrated in the energy range $0.5 T_e \leq h\nu \leq 5 T_e$.

The nonrelativistic $e-e$ bremsstrahlung is given by Maxon and Corman³⁴ as

$$P_{Bee} = 7.098 \times 10^{-21} n_e^2 (T_e)^{1/2} \frac{T_e}{mc^2} \quad (\text{keV/m}^3 \cdot \text{s}),$$

where $mc^2 = 512$ keV. Each impurity ion will have its associated radiation term and all radiation terms must be summed. Thus, the total nonrelativistic bremsstrahlung radiation power is

$$P_B = 3.346 \times 10^{-21} n_e^2 (T_e)^{1/2} (Z_{\text{eff}} + 0.00414 T_e),$$

$$\text{where } Z_{\text{eff}} = \sum n_i Z_i^2 / n_e.$$

Additional corrections need to be introduced in the relativistic region ($T_e \gtrsim 50$ keV) according to Maxon,³⁵ who gives expressions for $e-i$ and $e-e$ bremsstrahlung in both the nonrelativistic and the extreme relativistic region. Maxon gives smooth curve extrapolations between the two limiting cases (non-relativistic, extreme relativistic) for a hydrogenic plasma. Gould³⁶ gives a relativistic expression which leads to

$$P_{Bei} = 3.346 \times 10^{-21} n_e^2 Z_{\text{eff}} (T_e)^{1/2} \\ \times (1 + 1.55 \times 10^{-3} T_e + 7.15 \times 10^{-6} T_e^2),$$

which involves a correction factor of $\sim 23\%$ at $T_e = 100$ keV but only $\sim 1.6\%$ at $T_e = 10$ keV.

The $e-e$ bremsstrahlung rate given by Gould is identical to the nonrelativistic expression of Maxon and Corman.³⁴ [Maxon's 1972 paper has a typographical error which makes it too large by a factor of $\sqrt{2}$ (Ref. 37)]. Gould also gives an additional correction to the Born approximation but this is

quite small for $T_e \gg 1$ keV ($\sim 0.07/T_e^{1/2}$ unless the plasma is quite impure).

The final expression for both $e\text{-}i$ and $e\text{-}e$ bremsstrahlung is then taken as

$$\begin{aligned} P_B = & 3.346 \times 10^{-21} n_e^2 (T_e)^{1/2} \\ & \times [Z_{\text{eff}}(1 + 1.55 \times 10^{-3} T_e + 0.715 \times 10^{-5} T_e^2) \\ & + 0.071(\sum Z_i^3 n_i/n_e)/T_e^{1/2} + 0.00414 T_e] \end{aligned}$$

which incorporates first-order $e\text{-}i$ relativistic and spin corrections, $e\text{-}e$ emission (nonrelativistic), and a Born correction. The total correction to the Spitzer formula amounts to 8% at 10 keV and 65% at 100 keV for a hydrogenic plasma. Kirillov et al.³⁸ give a correction to the electron ion bremsstrahlung for incompletely stripped ions.

Cyclotron (Synchrotron) Radiation

Electrons moving perpendicular to a magnetic field are accelerated and execute gyro-orbits. The acceleration of a charged particle results in emission of electromagnetic radiation. Numerous attempts at evaluating the resultant cyclotron radiation loss utilize a locally applied global model (LAGM) (e.g., Yang et al.,³⁹ Rose,⁴⁰ and Trubnikov⁴¹) with results that show significant differences in radiation power loss. Tamor⁴² has done a comprehensive transport analysis of the problem for cylindrical and toroidal plasma shapes and finds that the plasma core radiates strongly but that the plasma is actually heated at large radii leading to a flatter temperature profile. He concludes that the LAGM models are remarkably good for predicting the *total* radiation loss at $T_e = 50$ keV but are inadequate to produce electron temperature profile effects and, in particular, core cooling. Thus, a full radiation transport calculation is essential.

The global models give for the cyclotron radiation power loss

$$P_C = 6.214 \times 10^{-20} n_e T_e B_T^2 \Phi \quad (\text{kW/m}^3),$$

where B_T is in Tesla, n_e is in m^{-3} , T_e is in kiloelectron volts, and Φ is the absorption correction summarized by Houlberg⁴³ as

$$\begin{aligned} \Phi_{\text{Yang}} = & \frac{1.94 \times 10^{-4}}{\Lambda^{1/2}} T_e^{1.1} [5 + 0.17(5 - A)]^3 \\ & \times (1 - R_\mu)^{1/2}, \end{aligned}$$

$$\Phi_{\text{Rose}} = \frac{1.402 \times 10^{-3}}{\Lambda^{1/2}} T_e^{1.75} \left(1 + \frac{T_e}{204}\right) (1 - R_\mu)^{1/2},$$

$$\Phi_{\text{Trubnikov}} = \frac{5.198 \times 10^{-3}}{\Lambda^{1/2}} T_e^{1.5} \left(1 + \frac{22.61}{AT_e^{1/2}}\right)^{1/2} \\ \times (1 - R_\mu)^{1/2},$$

and

$$\Lambda^{1/2} = 7.78 \times 10^{-9} \frac{n_e^{1/2} a^{1/2}}{B_T^{1/2}},$$

where a is the plasma radius in metres, A is the aspect ratio of the toroid = R/a , and R_μ is the wall reflectivity. The value of $\Phi/(1 - R_\mu)^{1/2}$ ranges from ~ 0.001 at 5 keV to about 0.1 at 100 keV. Values of R_μ for smooth metallic walls usually exceed 0.99; however, wall deterioration and penetrations may reduce this to ~ 0.9 . Corrections for plasma diamagnetism are usually approximated by substituting the expression $B_T(1 - \beta)^{1/2}$ for the vacuum field B_T where β is $2\mu_0 \Sigma n T / B_T^2$.

Rose's expression for Φ includes a first-order relativistic correction and gives a low estimate at low temperatures (< 50 keV) but is significantly higher at high electron temperatures. Etzweiler et al.⁴⁴ used twice Rose's coefficient which ensures better matching at low temperatures—this gives overconservatism in evaluating the cyclotron radiation losses at the higher temperatures. Full transport calculations appear to be necessary to obtain proper evaluations of the temperature profile effects and thus the detailed plasma reactivity.

PHYSICS FACTORS AFFECTING THE T_i/T_e RATIO

An increase in the ratio of T_i/T_e will lead in most cases to increased fusion reaction power compared to the radiation power loss. Since this will affect the operating temperature of Fig. 3, the resulting increased ion temperature and reaction power output will also drive the electron temperature somewhat higher to establish a new equilibrium operating temperature in which radiation power again equals fusion power. In addition, particle and energy losses may be decreased at the more elevated temperatures (neoclassical losses vary usually as $1/\sqrt{T}$). We examine several physics areas affecting the fusion burn properties of a reactor grade plasma.

It is important to note that the electrons which are moving slower than the ions "dominate" the Coulomb drag process in energy transfer from ions to electrons.⁴⁵ An electron having v_e just above v_i has $\sim 1\%$ as much stopping power as one having $v_e < v_i$. Figure 7 illustrates the energy transfer from an ion of velocity $v_i = 2 \times 10^8$ cm/s to electrons of speed v_e in a Maxwellian distribution of electrons at 10 keV. [Note that the number density of slow electrons in a Maxwellian distribution increases approximately as v_e^2 when $\frac{1}{2} mv_e^2 \ll 10$ keV, i.e., $f(v_e) \propto v_e^2$ for $v_e^2 < 0.1 v_i^2$.]

Rosenbluth Correction

About 20 years ago Rosenbluth derived an expression for the net depletion of the cold electrons

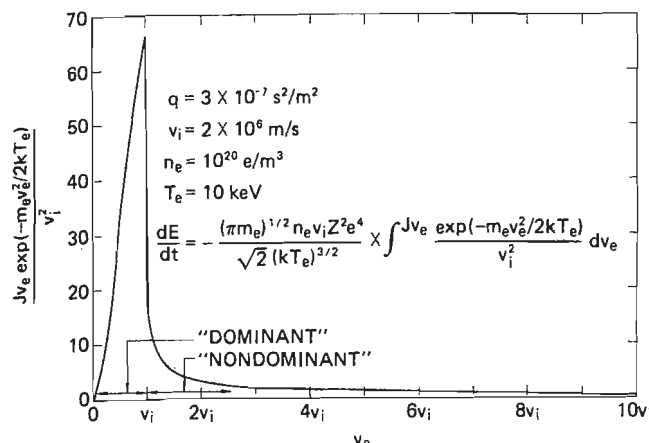


Fig. 7. Energy transfer from an ion to electrons of speed v_e in a Maxwellian sea of electrons at $T_e = 10$ keV. Note that the dominant energy loss is to electrons that are *slower* than the test ion.

in the toe of the Maxwellian electron distribution due to this selective electron heating by the ions at temperature T_i , corrected for the scattering of electrons back into the toe region. This result was eventually published and gave the correction to the Spitzer slowing down rate for the ions as⁴⁶

$$\left(\frac{dE}{dt}\right)_{ie} = \left(\frac{dE}{dt}\right)_{Spitzer} \times \left[1 - \left(\frac{2\pi^2}{3^{5/4}} \frac{m_e Z T_i}{m_i T_e}\right)^{2/3}\right]$$

and amounts to a few percent in most cases. Table IX shows the effect on a marginally ignited but steady-state catalyzed D-D plasma. Thus, a 1.6% depletion of cold electrons can lead to an ~11% increase in power output. Both T_i and T_e show increases with the former increase more marked.

Magnetic Field Correction to Stopping Power

In strong magnetic fields such as those encountered in fusion reactor plasmas, the stopping power of electrons on the ions (fast or thermal) is reduced because of a reduction in the maximum impact parameter for Coulomb collisions.⁴⁷ Figure 8 indicates the physics of the process whereby one of the slow electrons experiences an $\xi \times B$ field and nutates about the direction of the test ion of velocity v_+ . An approximate maximum impact parameter is given by $v_+/\sqrt{2}\omega_{ce}$, where ω_{ce} is the electron gyro-frequency. This may be smaller than the Debye polarization distance λ_D , and thus the Coulomb logarithm ($\ln \lambda_D 3kT_e/Ze^2$) in the test ion slowing down problem is reduced. Table X illustrates the magnetic field effect correction (B effect) for a catalyzed D-D burn—one notes almost 50% more power output.

TABLE IX
Effect of Rosenbluth Correction (RC) for Depletion of Cold Electrons in Steady-State Catalyzed D-D Plasmas*

| RC | T_i (keV) | T_e (keV) | β (%) | P_{total} (kW/m ³) |
|-------------------------|----------------|----------------|----------------|-------------------------------------|
| No (1.0) Yes (0.984) | 93.4 | 69.1 | 23.7 | 294 |
| | 103.0 | 73.2 | 25.6 | 326 |
| Effect of RC (%) | | | | |
| | +10.3 | +5.9 | +8.0 | +10.9 |

* $B = 5.0$ T, $R_\mu = 0.9$, $a = 5\text{-m o.d.}$, $n_e = 1.0 \times 10^{20}$ m⁻³, and $n_d/n_e = 0.55$. Plasma is marginally ignited.

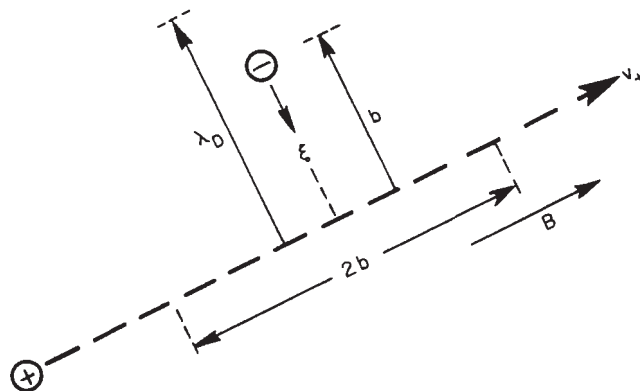


Fig. 8. Bohr-Fermi method of analyzing maximum impact parameter for test ion moving at velocity v_+ in an electron sea immersed in a magnetic field B . When the Debye distance λ_D is larger than $v_+/\omega_{ce}\sqrt{2}$, the latter defines an approximate maximum impact parameter. The mean electric field is $\xi \approx Ze/b^2$, and the approximate collision time is $2b/v_+$.

The Rosenbluth correction has less influence in the example of Table X than Table IX because of the higher deuterium density; other effects shown are nuclear scattering and the proton burning reaction ($p_{fast} + T \rightarrow n + {}^3He - 0.8$ MeV) due to fast protons reacting with tritium during their slowing down as well as reactions by the few fast protons in the thermal distribution.

Nuclear Elastic Corrections

The application of nuclear elastic collision effects in promoting the mean energy of the ions in a plasma for controlled fusion applications was apparently first made⁴⁸ in 1975. Figure 9 shows a few of the nuclear elastic slowing down rates for charged particles with deuterons⁴⁹ along with a rough average

TABLE X
Corrections to Catalyzed D-D Burns*

| Parameter | Catalyzed D-D | Plus B Effect | Plus RC | Plus NS ^a | Plus p + T |
|---------------------------------------|---------------|---------------|---------|----------------------|------------|
| T_i (keV) | 100 | 143 | 144 | 173 | 175 |
| T_e (keV) | 82 | 95 | 96 | 101 | 102 |
| β (%) | 27.3 | 35.3 | 35.5 | 40.3 | 40.7 |
| P_{CHP} (kW/m ³) | 235 | 334 | 337 | 397 | 407 |
| P_{NAB} (kW/m ³) | 209 | 296 | 299 | 352 | 351 |
| n_T/n_e | 0.0088 | 0.0140 | 0.0142 | 0.0181 | 0.0178 |

* $n_e = 10^{20} \text{ m}^{-3}$, $n_p/n_e = 0.65$, $B_0 = 5 \text{ T}$, $R_\mu = 0.9$, $a = 5 \text{ m}$, $\tau_E = \tau_p$. P_{CHP} = power in charge particles; P_{NAB} = power in neutrons and blanket energy release (blanket energy release taken as 4.8 MeV/n).

^aNS = nuclear scatter effect.

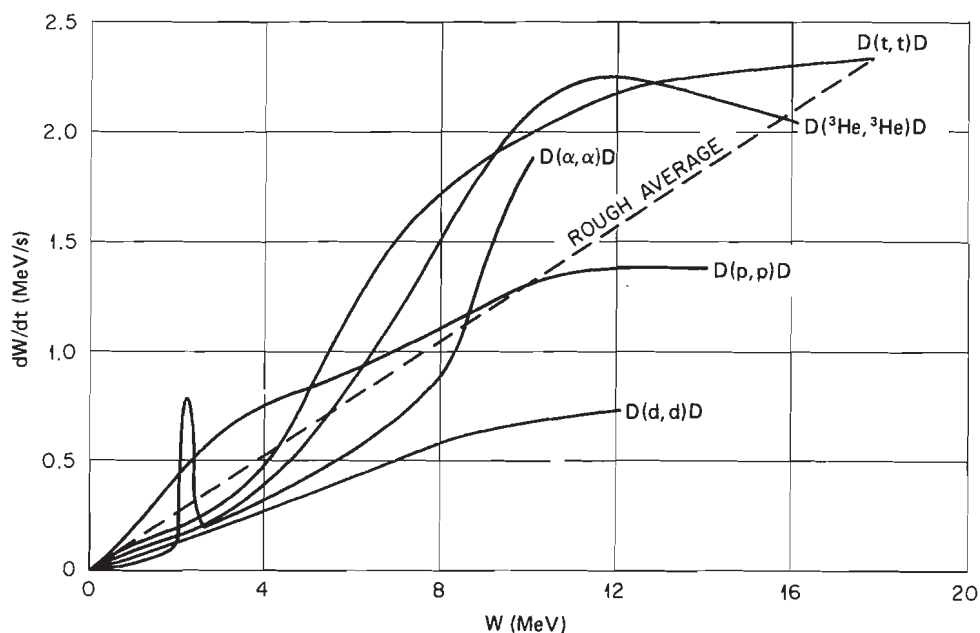


Fig. 9. Energy loss rates for nuclear elastic collisions with deuterons (after Ref. 49).

used to make an approximate evaluation of the net energy transfer to the plasma ions. A comparison of this average rate with Coulomb slow-down rates for test ions on deuterons and electrons is given in Fig. 10. Note that the total power feed from fast ions to thermal ions is comparable to that to the electrons at $T_e = 100 \text{ keV}$. More recent and much more complete nuclear elastic scattering data are now available.⁵⁰ Table X shows the significant increase in plasma reactivity due to nuclear elastic corrections.

Proton Consumption in Fusion Reactors

The conversion of fast protons and thermal tritons to neutrons and ^3He nuclei proceeds via the

reaction listed above and also in Table I. Although some reactive tritium is lost, (relatively) slow neutrons instead of 14-MeV neutrons are produced. In addition, the proton- and energy-rich ^3He nuclide is generated which can deposit five times as much charged-particle reaction energy in the plasma in reacting with deuterons as can a triton. Although the burnup rate for D- ^3He is lower than that for D-T, one still gains a slight plasma reactivity, as indicated in Table X.

Possible Diffusion Effects in Magnetic Fields

Inasmuch as normal particle diffusion processes in magnetic fields lead to a preferential loss of low

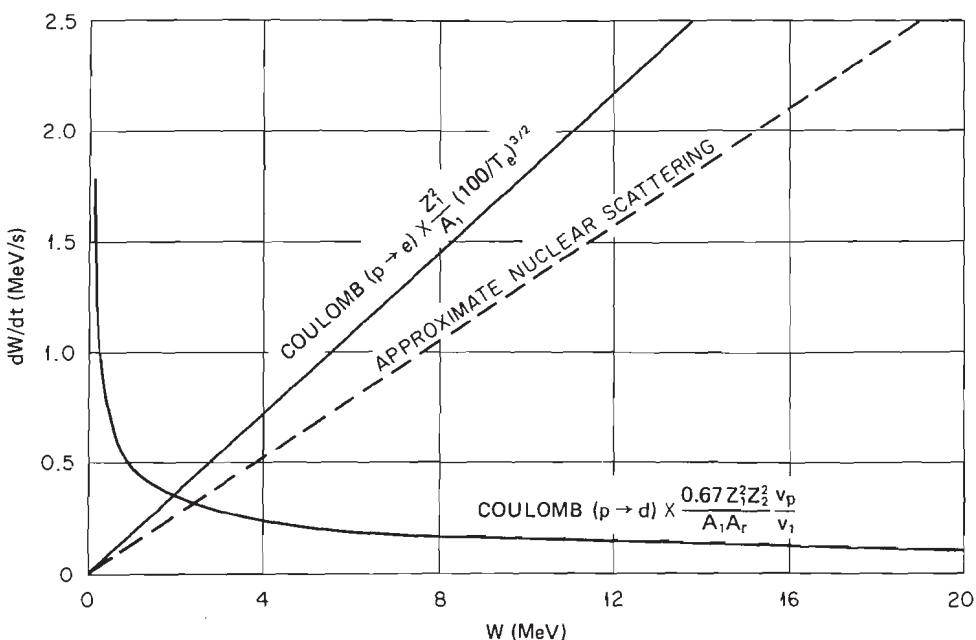


Fig. 10. Comparison of nuclear elastic and Coulomb energy loss rates in deuterium plasma at $n_e = n_d = 10^{20} \text{ m}^{-3}$; 1 designates test ion, A = atomic mass number, and A_r = reduced atomic mass number.

energy particles ($\tau_{\text{mirror}} \propto v^3$; $\tau_{LB} \propto v$), there may be a significant hardening of the energy spectrum of the remaining trapped particles. Diffusion of ions and electrons back into the low speed region of the distributions will tend to offset this loss process but can lead to a reduced stopping power of the remaining electrons on the trapped ions since the distribution is somewhat depleted in the region of dominant energy transfer ($v_e \leq v_i$). This simulated Maxwell-demon effect has apparently not been considered in detail but the Fokker-Planck studies of Futch et al.⁵¹ may suggest such an effect in operation in magnetic mirrors containing reacting plasmas. However, the observed results are complicated by the Rosenbluth effect, the cold electron input, the ambipolar diffusion, and possibly other perturbing influences.

Plasma Flow Effects

A number of interesting plasmas have exhibited marked plasma flows or quasi-solid body rotation (e.g., see Ref. 52) as well as $\xi \times B$ drifts. This introduces a center-of-mass motion of both ions and electrons that, for part of the ion gyro-orbit (i.e., when $v_{\text{flow}} \parallel v_{thi}$), can tend to a substantial increase in the collisional energy of ion pairs. The effect on the electrons may be minimal since v_{flow} is generally very much less than the average electron speed. In the reactor regime v_{flow} may exceed about 10^6 m/s but should it approach or exceed 10^7 m/s it might per-

haps have a major impact. Suckewer et al.⁵² have observed toroidal flow velocities up to 10^5 m/s in the moderate temperature, beam-driven PLT plasma, but they have projected⁵² 10^6 m/s for the larger size TFTR. Whether plasma flows can affect the ion-ion scattering and reaction rates as well as the ion-electron energy interchange has apparently not been evaluated.

Other Nuclear Effects

In general, nuclear elastic and hard Coulomb scattering of fuel ions by fast reaction products leads to suprathermal fuel ions which can react faster and hence can increase the plasma power output. Shuy and Conn have referred to this effect as tail-tail interactions.¹² This may supplement any chain reaction features (e.g., as in $p-{}^6\text{Li}$) and is itself a chaining process.

As an extreme example, five 3-MeV protons (which might be elevated out of the thermal distribution by nuclear elastic or hard Coulomb collisions by one 15-MeV proton) have a total chaining effect three times larger than that of one 15-MeV proton in driving the reaction $p_{\text{fast}} + {}^6\text{Li} \rightarrow {}^3\text{He} + {}^4\text{He}$ as the protons slow down into the thermal distribution (see Fig. 6). Fokker-Planck studies are essential to the proper evaluation of the details of such large energy transfer processes.

Nuclear dissociation events (e.g., $X + {}^6\text{Li} \rightarrow X' + {}^6\text{Li}^* - 2.184 \text{ MeV} \rightarrow X' + d + \alpha - 1.471 \text{ MeV}$; see

Fig. 6) and the excitation of gamma emitting levels (e.g., $X + {}^7\text{Li} \rightarrow X' + {}^7\text{Li}^* - 0.478 \rightarrow X' + {}^7\text{Li} + h\nu - 0.478 \text{ MeV}$) can degrade the fusion burn because of the associated energy loss from the plasma and possible change in the fuel/ash mix ratio. Nuclear energy level schemes for the light elements along with detailed nuclear information and references are reported by Ajzenberg et al.^{32,53} Nuclear mass-energy resonance reactions based on these latter references have been outlined by McNally⁵⁴ who pointed out the strong resonance involving 622-keV protons in the p-¹¹B reaction, among others. The partition of reactant nuclei among excited states may lead to increased reactivity in very thick plasmas,⁵⁵ whereas the production of excited nuclear states as a result of resonance reactions might lead to a gamma-driven fusion burn¹⁴ but only in very thick plasmas. Energetic (~ 17 -MeV) gamma-ray production in the D-T and D-³He mass-energy resonance reactions occurs in about $\frac{1}{5000}$ and $\frac{1}{14000}$ of the reactions, respectively (consult Refs. 32 and 53 for gamma-producing nuclear energy levels).

Ion Cyclotron Instability Effects

Ion cyclotron resonance heating (ICRH) has been successfully demonstrated principally via heating of minority species (e.g., protium in deuterium plasmas) with subsequent collisional heating of the majority species.⁵⁶ In a reacting plasma there may be *in situ* ICRH coupling between energetic fusion product ions and the fuel ions, especially if coherent bunching of ions occurs. This might lead to a more rapid energy transfer to the fuel ions (especially deuterons from alpha particles since $Z/A = \frac{1}{2}$ in both cases; other harmonics than the fundamental may drive additional heating modes since $Z/A = 1, \frac{1}{2}, \frac{1}{3}, \frac{2}{3}$, and $\frac{1}{2}$ for p, d, t, ³He²⁺, and ⁴He²⁺, respectively). An in depth study of possible *in situ* ICRH coupling may reveal a faster mode of energy transfer from the fusion product ions to the fuel ions than via simple Coulomb collision processes. Such an effect would lead to some increase in T_i/T_e as shown in Ref. 25, which would further improve the prospects of the advanced fusion fuels.⁵⁷

Powerful examples of the strong cyclotron resonance coupling between a small class of organized quasi-monoenergetic protons with other protons were found in the DCX series of experiments at ORNL many years ago. The negative mass instability driven by a few recently trapped 300-keV protons in DCX-1 led to a gross spreading of the energy spectrum of all the trapped protons which led to serious losses due to large orbits and spatial spreading as well as to increased charge-exchange losses for the lower energy down-scattered particles.⁵⁸ On turnoff of the injection beam (and hence of the recently trapped, well-organized particles), the plasma became spectacularly quiescent, with classical charge-exchange losses of the

spread population being the dominant loss process. Confinement times up to 150 s were obtained in these low density DCX-1 plasmas. The more rapid Lorentz trapping (compared with the slower proton trapping on neutral background gas and plasma particles) drove the instability harder. In DCX-2 cyclotron harmonics up to more than 50 were observed, and the resultant trapped and spread population driven by a modified negative mass instability produced an average ion energy almost double the injection proton energy due to the steep energy dependence of the charge exchange with the resultant spread distribution.⁵⁹ Thus, even in low density, energetic ion plasmas ($n_i \lesssim 5 \times 10^{15} \text{ m}^{-3}$) coherent bunching of a small energetic ion population may lead to large energy transfers, rapid energy spreading, and energy spectrum hardening in the background ion population via cyclotron-type resonances and selective low energy loss processes.

CONCLUSIONS

Considerable progress has been made in our understanding of the physics of burning fusion fuels. It would appear that more emphasis should be given to incorporating additional nuclear phenomena in fusion burn studies since these will play a dominant role in an ultimate fusion economy. The D-D fusion fuel prospects appear to offer the highest potential for a viable fusion (and possibly fission) reactor economy.

ACKNOWLEDGMENTS

I am indebted to Johnnie Cannon and F. W. Wiffen for several helpful suggestions, to R. A. Dory for encouragement in the preparation of this manuscript, to W. A. Houlberg for suggestions and a review of the manuscript, and to K. E. Rothe for numerous contributions pertaining to advanced fuels studies.

This paper is based in part on an invited paper presented at the 1981 IEEE International Conference on Plasma Science, Santa Fe, New Mexico, May 18-20, 1981. The research was sponsored by the U.S. Department of Energy, Office of Fusion Energy, under Contract No. W-7405-eng-26 with the Union Carbide Corporation.

REFERENCES

1. J. C. MARK, "Report on Conference on the Super," LA-575, Los Alamos National Laboratory (June 1946), sanitized version (May 1971); see also "A Short Account of Los Alamos Theoretical Work on Thermonuclear Weapons, 1946-1950," LA-5647-MS, Los Alamos National Laboratory (1974).

2. Proc. Second United Nations Int. Conf. Peaceful Uses of Atomic Energy, Geneva, Switzerland, September 1-13, 1958, Vols. 31-33, United Nations (1958).
3. C. C. BAKER, G. A. CARLSON, and R. A. KRAKOWSKI, "Trends and Developments in Magnetic Confinement Fusion Reactor Concepts," *Nucl. Technol./Fusion*, **1**, 5 (1981).
4. H. A. BETHE, *Phys. Today*, **21**, 36 (1968).
5. J. R. McNALLY, Jr., K. E. ROTHE, and R. D. SHARP, "Fusion Reactivity Graphs and Tables for Charged Particle Reactions," ORNL/TM-6914, Oak Ridge National Laboratory (1979). Updated tables containing $\langle\sigma v\rangle$ data for 37 reactions are available from the first author.
6. R. J. HOWERTON, "Maxwell-Averaged Reaction Rates ($\overline{\sigma v}$) for Selected Reactions Between Ions with Atomic Mass ≤ 11 ," UCRL-50400, Vol. 21, Part A, Lawrence Livermore National Laboratory (1979). Report contains data for 24 reactions.
7. D. STEINER, "The Technological Requirements for Power by Fusion," *Nucl. Sci. Eng.*, **58**, 107 (1975).
8. R. G. MILLS, "Catalyzed Deuterium Fusion Reactors," PPL-TM-259, Princeton Plasma Physics Laboratory (1971).
9. J. R. McNALLY, Jr., *Nucl. Fusion*, **11**, 189 (1971).
10. T. WEAVER, G. ZIMMERMAN, and L. WOOD, "Prospects for Exotic Thermonuclear Fuel Usage in CTR Systems," UCRL-74191, UCRL-74352, Lawrence Livermore National Laboratory (1972); see also "Exotic CTR Fuels: Non-Thermal Effects and Laser Fusion Applications," UCRL-74938, Lawrence Livermore National Laboratory (1973).
11. J. R. McNALLY, Jr. and K. E. ROTHE, Oak Ridge National Laboratory, Private Communication (1980).
12. G. W. SHUY and R. W. CONN, "Physics Phenomena in the Analysis of Advanced Fusion Fuel Cycles," PPG-522, University of California, Los Angeles (1980); see also "Charged Particle Cross Section Requirements for Advanced Fusion Fuel Cycles," *Proc. Int. Conf. Nuclear Cross Sections for Technology*, NBS Special Publication 594, p. 254, U.S. National Bureau of Standards (1980).
13. G. H. MILEY, "Advanced Fuels and the Development of Fusion Power," FSL-54, University of Illinois (1981); see also "Potential and Status of Alternate-Fuel Fusion," COO-2218-175, University of Illinois (1980).
14. J. R. McNALLY, Jr., "Gamma-Driven Fusion Burns," unpublished.
15. J. M. DAWSON, H. P. FURTH, and F. H. TENNEY, *Phys. Rev. Lett.*, **26**, 1156 (1971).
16. J. R. McNALLY, Jr., *Nucl. Fusion*, **17**, 1273 (1977); see also "A Simple Measure of Merit for Fusion Feasibility," ORNL/TM-6362, Oak Ridge National Laboratory (1978).
17. J. D. LAWSON, *Proc. Phys. Soc. London B*, **70**, 6 (1957).
18. C. C. BAKER et al., "STARFIRE—A Commercial Tokamak Fusion Power Plant Study," ANL/FPP-80-1, Argonne National Laboratory (1980).
19. W. STODIEK et al., *Proc. Eighth Int. Conf. Plasma Physics and Controlled Nuclear Fusion Research*, Brussels, Belgium, July 1-10, 1980, International Atomic Energy Agency (to be published).
20. T. C. SIMONEN et al., *Proc. 7th Int. Conf. Plasma Physics and Controlled Nuclear Fusion Research*, Innsbruck, Austria, August 23-30, 1978, Vol. II, p. 389, International Atomic Energy Agency (1979).
21. T. C. SIMONEN, Ed., "Summary of TMX Results—Executive Summary," UCRL-53120 Summary, Lawrence Livermore National Laboratory Tandem Mirror Experiment (1981).
22. L. R. GRISHAM, *Science*, **207**, 1301 (1980).
23. R. TOSCHI, Centro di Frascati, Private Communication (Sep. 1981).
24. J. G. CORDEY, in *Theory of Magnetically Confined Plasmas: Proc. Course and Workshop*, Varenna, Italy, 1977, p. 307, Pergamon Press (1979).
25. J. F. CLARKE, *Nucl. Fusion*, **20**, 563 (1980).
26. C. A. FLANAGAN, D. STEINER, and G. E. SMITH, Eds., "The Initial Trade and Design Study for the Fusion Engineering Device," ORNL/TM-7777, Oak Ridge National Laboratory (1981); see also "Fusion Engineering Device Mission and Program Summary," DOE/TIC-11600, Vol. 1, U.S. Department of Energy (1981), see also Vols. 2 through 6.
27. M. J. SALTMARSH, W. R. GRIMES, and R. T. SANTORO, ORNL/PPA-79/3, Oak Ridge National Laboratory (1979).
28. J. R. McNALLY, Jr., *Nucl. Fusion*, **18**, 133 (1978).
29. J. R. McNALLY, Jr., *Nucl. Fusion*, **11**, 187 (1971). For a general discussion of fusion chain reactions see "Fusion, Nuclear" in *Encyclopedia of Chemistry*, 3rd ed., Van Nostrand Reinhold Company, New York (1973).
30. L. RUBY and T. P. LUNG, "Effect of $^6\text{Li} + ^6\text{Li}$ Reactions in a Fusion Reactor Operating on $^6\text{Li}(p,\alpha)^3\text{He}$," *Nucl. Sci. Eng.*, **69**, 107 (1979).
31. J. R. McNALLY, Jr. and K. E. ROTHE, *Int. Conf. Plasma Science Abstracts*, 79CH1410-0 NPS, p. 52, Institute of Electronics and Electrical Engineers (1979).
32. F. AJZENBERG-SELOVE, *Nucl. Phys. A*, **320**, 1 (1979).
33. L. J. SPITZER, Jr., *Physics of Fully Ionized Gases*, Wiley-Interscience Publishers, New York (1962).
34. M. S. MAXON and E. G. CORMAN, *Phys. Rev.*, **163**, 156 (1967).

35. S. MAXON, *Phys. Rev. A*, **5**, 1630 (1972).
36. R. J. GOULD, *Astrophys. J.*, **238**, 1026 (1980). The coefficient of the third term of Eq. (41) apparently should be $5/24\sqrt{2}$ rather than $5/8\sqrt{2}$.
37. S. MAXON, Lawrence Livermore National Laboratory, Private Communication (1981).
38. V. D. KIRILLOV, B. A. TRUBNIKOV, and S. A. TRUSHIN, *Sov. J. Plasma Phys.*, **1**, 117 (1975).
39. T. F. YANG, H. K. FORSEN, and G. A. EMMERT, UWFDM-49, University of Wisconsin (1973).
40. D. J. ROSE, "On the Feasibility of Power by Nuclear Fusion," ORNL/TM-2204, Oak Ridge National Laboratory (1978); see also *Nucl. Fusion*, **9**, 183 (1969).
41. B. A. TRUBNIKOV, *J. Exp. Theor. Phys.*, **16**, 1 (1972).
42. S. TAMOR, "Studies of Emission and Transport of Synchrotron Radiation in Tokamaks," LAPS-71, SAI-023-81-110LJ, Science Applications, Inc. (1981).
43. W. A. HOULBERG, Oak Ridge National Laboratory, Private Communication (1981).
44. J. F. ETZWEILER, J. F. CLARKE, and R. H. FOWLER, "Effect of Fuel Injection on a Cyclic β -Limited Radiation Dominated Fusion Reactor," ORNL/TM-4083, Oak Ridge National Laboratory (1973).
45. J. R. McNALLY, Jr., "Energy Transfer from Ions to Electrons and the Coulomb Logarithm," ORNL/TM-5803, Oak Ridge National Laboratory (1977). Note: Coefficient on line 10, p. 5 should be $\sqrt{16/9\pi}$ not $\sqrt{16/\pi}$.
46. M. ROSENBLUTH, *Bull. Am. Phys. Soc.*, **21**, 1114 (1976).
47. J. R. McNALLY, Jr., *Nucl. Fusion*, **15**, 344 (1975).
48. J. R. McNALLY, Jr., *Proc. Conf. Nuclear Cross Sections and Technology*, NBS Special Publication 425, **2**, 683, U.S. National Bureau of Standards (1975); see also *Proc. 6th IEEE Symp. Engineering Problems of Fusion Research*, p. 1012, Institute of Electronics and Electrical Engineers (1976).
49. J. J. DEVANEY and M. L. STEIN, "Plasma Energy Deposition from Nuclear Elastic Scattering," *Nucl. Sci. Eng.*, **46**, 323 (1971); p, d, t, ^3He , ^4He on d.
50. S. T. PERKINS and D. E. CULLEN, "Elastic Nuclear Plus Interference Cross Sections for Light-Charged Particles," *Nucl. Sci. Eng.*, **77**, 20 (1981); p, d, t, ^3He , ^4He with each other; see also UCRL-50400, Vol. 15, Part F, Lawrence Livermore National Laboratory (1980).
51. A. H. FUTCH, Jr., J. P. HOLDREN, J. KILLEEN, and A. A. MIRIN, *Plasma Phys.*, **14**, 211 (1972).
52. S. SUCKEWER, H. P. EUBANK, R. J. GOLDSTON, J. McENERNY, N. R. SAUHOFF, and H. H. TOWNER "Toroidal Plasma Rotation in the PLT Tokamak with Neutra Beam Injection," PPPL-1792, Princeton Plasma Physics Laboratory (1981).
53. F. AJZENBERG et al., *Nucl. Phys. A*, **268**, 1 (1976); see also *Nucl. Phys. A*, **281**, 1 (1977); see also *Nucl. Phys. A*, **336**, 1, 113 (1980).
54. J. R. McNALLY, Jr., "Nuclear Fusion Resonance Reactions of Possible CTR Interest," ORNL/TM-3233, Revised Oak Ridge National Laboratory (1971).
55. N. A. BAHCALL and W. A. FOWLER, *Astrophys. J.*, **157**, 645 (1969); see also *Astrophys. J.*, **161**, 119 (1970).
56. J. HOSEA et al., *Proc. 8th Int. Conf. Plasma Physics and Controlled Nuclear Fusion Research*, Brussels, Belgium, Jul 1-10, 1980, International Atomic Energy Agency (to be published).
57. J. H. SCHULTZ, L. BROMBERG, and D. R. COHN, *Nuc Fusion*, **20**, 703 (1980).
58. H. POSTMA, J. L. DUNLAP, R. A. DORY, G. R. HASTI and R. A. YOUNG, *Phys. Rev. Lett.*, **16**, 265 (1966); see also J. L. DUNLAP, G. R. HASTE, C. E. NIELSEN, H. POSTMA, and L. H. REBER, *Phys. Fluids*, **9**, 199 (1966).
59. P. R. BELL, R. A. DORY, G. E. GUEST, G. G. KELLEY, N. H. LAZAR, J. F. LYON, and R. F. STRATTON, *Phys. Rev. Lett.*, **16**, 1152 (1966); see also J. F. CLARKE, G. G. KELLEY, J. F. LYON, and R. F. STRATTON, *Proc. 3rd Int. Conf. Plasma Physics and Controlled Nuclear Fusion Research*, Novosibirsk, August 1968, **2**, 291, International Atomic Energy Agency (1969).

Note Added in Proof: Recent $p-^{11}\text{B}$ studies incorporating more exact nuclear elastic scattering effects indicate that it will not ignite over radiation loss (J. D. Gordon et al., " $p-^{11}\text{B}$ Multiple Evaluation presented at Third IAEA Technical Committee Meeting and Workshop on Fusion Reactor Design and Technology, Tokyo, Japan, October 5-16, 1981).